



Partitioning And Transmuter Research Initiative in a Collaborative Innovation Action

PATRICIA

Grant Agreement Number 945077

Research and Innovation Action

Activity: NFRP-2019-2020

Topic: NFRP-2019-2020-07 Safety Research and Innovation for Partitioning and/or Transmutation

Start date: 01/09/2020 – Duration: 48 months

DELIVERABLE

D5.2 Description of new meso-scale models and their implementation in fuel performance codes

**Authors: A. Magni, M. Di Gennaro, D. Pizzocri, G. Zullo, L. Luzzi (POLIMI), M. Lainet (CEA),
A. Schubert, P. Van Uffelen (JRC)**



This project has received funding from the European Union's Horizon 2020 research and innovation programme under grant agreement No 945077.

DOCUMENT CONTROL SHEET

DOCUMENT INFORMATION

Document title	Description of new meso-scale models and their implementation in fuel performance codes
Author(s), (organization)	A. Magni, M. Di Gennaro, D. Pizzocri, G. Zullo, L. Luzzi (POLIMI), M. Lainet (CEA), A. Schubert, P. Van Uffelen (JRC)
Document type	Deliverable
Document ID	D5.2
Work package n°	WP5 (Domain: Transmutation)
Work package title	WP5 (WP22) Improvement of modelling and fuel performance codes
Lead beneficiary	POLIMI
Dissemination level	Public
Date of issue	07/08/2023
Archive ID reference COO	SCK CEN/56669139

DOCUMENT SUMMARY

This deliverable illustrates the new (2.0) version of the SCIANTIX meso-scale code, developed within Task 5.2 of the PATRICIA Project, highlighting first the code structure and its numerical features. Then, the SCIANTIX models for various physics involved in the inert gas behaviour are described in detail along with their corresponding separate-effect validation database and validation results. The coupling of SCIANTIX with integral, pin-level fuel performance codes is also introduced, presenting the different strategy and interface details for the coupling with the TRANSURANUS and GERMINAL fuel performance codes. Finally, conclusions and future perspectives are provided, mentioning several envisaged developments targeted in the framework of multiple research initiatives at a European and international level, and outlining the strategy foreseen for further developments of the code (in both its stand-alone and coupled fashion).

DOCUMENT HISTORY

Version	Status	Date
v0	Draft	21/07/2023
v1	Final	07/08/2023

DOCUMENT APPROVAL

The author, WP Leader and Coordinator acknowledge and accept delivery of the work completed for this deliverable.

Date	Author(s)	Organisation
21/07/2023	Alessio Magni, Martina Di Gennaro, Davide Pizzocri, Giovanni Zullo, Lelio Luzzi Marc Lainet Arndt Schubert, Paul Van Uffelen	POLIMI CEA JRC
Date	WP Leader	Organisation
24/07/2023	Lelio Luzzi	POLIMI
Date	Coordinator	Organisation
07/08/2023	Paul Schuurmans 	SCK CEN

DISTRIBUTION LIST

Project Officer Renata Bachorczyk-Nagy	EC	Copy on PATRICIA SharePoint
PATRICIA Beneficiaries	PATRICIA Consortium	

Table of contents

1	Introduction.....	5
2	Structure and numerical features of SCIANTIX 2.0	8
3	Inert gas behaviour modelling in SCIANTIX	10
3.1	Helium production from burnup module capabilities.....	11
3.1.1	Methodology	12
3.1.2	Surrogate model for fast reactor conditions.....	15
3.1.3	Surrogate model for MYRRHA irradiation conditions	20
3.2	Helium behaviour	25
3.2.1	Intra-granular helium behaviour	25
3.2.2	Consideration of the intra-granular behaviour of cocktails of inert gases.....	27
3.2.3	Inter-granular helium behaviour	28
3.2.4	Effect of grain size distribution on helium behaviour	29
4	Coupling of SCIANTIX with fuel performance codes	32
4.1	Coupling of SCIANTIX with TRANSURANUS.....	33
4.2	Coupling of SCIANTIX with GERMINAL	35
5	Conclusions.....	38
6	References.....	39

1 Introduction

Understanding and predicting the behaviour of inert gases in nuclear fuel is vital to ensure a reliable, efficient and overall safe operation of fuel rods in both light water-cooled and fast reactors [1]–[4]. Physics-based approaches based on kinetic rate-theory models [5]–[11], and corresponding codes and tools (e.g., MFPR [12], [13], CARACAS [14], MARGARET [15], VICTORIA [16], FASTGRASS [17]), have been developed to capture the intricate inert gas behaviour (IGB) in nuclear fuel. The use of kinetic rate-theory models is motivated by several inherent advantages:

- Description relying on a limited set of governing differential equations for the different gas-related phenomena [7], [18], [19].
- Natural application of the simulation to a wide range of operational and accidental transient scenarios [6], [13], [20].
- Direct benefit from new separate-effect experimental data available, hence extending the separate-effect validation database of the implemented models [21]–[23].
- Bridging information from lower-length scales (e.g., by definition of specific model parameters [24]–[30]) to engineering scale of the nuclear fuel rod, easing the applicability to different fuel materials (e.g., by modifying specific material properties) with minor modifications.

Among the mentioned (reported in literature) meso-scale codes dealing with physics-based IGB modelling, none are open-source, hindering their applicability in the frame of multi-scale and multi-physical nuclear fuel analysis involving different software packages [31]. Therefore, SCIANTIX [32] was developed with the goal of being an open-source, standalone code for IGB physics-based modelling, applicable to simulations of experiments with separate effects on the fuel grain scale, or generally to samples in uniform conditions, supporting both the design of the experiment itself and the interpretation of the results.

SCIANTIX is currently available as an open-source code under MIT license, greatly easing its usage as IGB module in existing fuel performance codes (FPCs). Because of this licensing choice, all the implemented models are already published and validated against separate-effect experiments. The choice of such license is a fundamental point for the application of SCIANTIX as IGB module, since FPCs are not typically available as open-source codes¹, and sharing developments within the context of collaborative international projects and educational initiatives can pose challenges. The integration of open-source tools like SCIANTIX within the FPC infrastructure offers a promising solution to this limitation. Given the open-source nature of SCIANTIX, standardised qualification and quality assurance guidelines are being considered and directly integrated in the source code and in its online repository (this activity is being targeted in the framework of the OperaHPC Euratom Project [33]). The code repository is available online at [34], [35], including the validation database of the implemented SCIANTIX models and non-regression testing tools and continuous integration services. These services are going to be further extended and developed, to improve the process of testing new code versions and branches, and also to clarify the guidelines for contributors.

At the engineering scale, FPCs are fundamental tools to predict the behavior of fuel pins, encompassing different operating conditions such as normal operation, accidental conditions and dry storage [3], [36], [45], [46], [37]–[44]. Notably, FPCs are currently being developed to enable multi-dimensional simulations (1D, 1.5D, 2D, 3D), which involves a physics-based modelling at the fuel grain scale by coupling with dedicated meso-scale modules [31], [47]–[49]. The coupling of FPCs with the SCIANTIX code has proven to be beneficial for the integral fuel rod simulation [50]–[54], since SCIANTIX is able to

¹ Some exceptions are worth mentioning, e.g., the OFFBEAT code [46], already coupled to SCIANTIX, and in general the ONCORE/IAEA involved codes [56], [126].

effectively bridge lower-length scale information (e.g., from experiments or molecular dynamics simulations) to the rod engineering scale, acting as physics-based IGB module within the FPC, with an emphasis on maintaining a limited computational time for the overall integral pin performance simulation. This allows to introduce more physics-based capabilities in FPCs, overcoming the correlation-based approach traditionally employed by legacy FPCs.

Connected to the PATRICIA Project activities, namely within Task 5.2, an advanced version (2.0) of the SCIANTIX code has been developed [55], targeting in particular models relevant for fast reactor fuel materials and conditions, i.e., the helium production and behaviour. Since its release [32], SCIANTIX has undergone recent and significant updates and advancements, preserving the original code capabilities but including the incorporation of new modelling and numerical features. The code architecture has been revamped, embracing an object-oriented structure improving the overall efficiency and usability [55], [56]. This Deliverable provides a concise overview of the current SCIANTIX code capabilities, in line with a new journal publication about SCIANTIX 2.0 [55]. SCIANTIX models relevant for application within PATRICIA are presented along with the corresponding separate-effect validation database, which is used to assess its accuracy and predictions. The SCIANTIX capabilities are available and coupled with FPCs by means of interface approaches and schemes, which are in place for GERMINAL and TRANSURANUS FPCs (involved in PATRICIA) or currently under development in the framework of several European Projects (e.g., R2CA [57], OperaHPC [33]).

The deliverable is structured as follows. Section 2 illustrates the SCIANTIX 2.0 code structure and its numerical features, while Section 3 generally recalls the SCIANTIX models for inert gas behaviour but focuses on the capabilities on helium relevant for fast reactor-type, mixed-oxide (MOX) fuels, providing the corresponding separate-effect validation database for each model and validation results. Section 4 introduces the coupling of SCIANTIX with integral FPCs, while the simulation results from the FPCs//SCIANTIX coupled suites will be the object of follow-up dedicated deliverables, i.e., D5.3 from Work Package 5 and D6.1 – D6.2 from Work Package 6. Section 5 draws conclusions about the achieved SCIANTIX modelling activities in support of the goals of the PATRICIA Project.

Table 1. Symbols used for the equations contained in the present deliverable.

Nomenclature		
$[^4\text{He}]$	Isotope concentration (e.g., of ^4He)	atoms m^{-3}
b	Intra-granular trapping rate	s^{-1}
c	Single-atom gas concentration	atoms m^{-3}
c_{lim}	Solubility	atoms m^{-3}
D	Intra-granular diffusivity	$\text{m}^2 \text{s}^{-1}$
\dot{F}	Fission rate density	fissions $\text{m}^{-3} \text{s}^{-1}$
g	Intra-granular irradiation-induced re-solution rate	s^{-1}
k_B	Boltzmann constant	J K^{-1}
k_H	Henry's constant	atoms $\text{m}^{-3} \text{MPa}^{-1}$
m	Gas concentration in intra-granular bubbles	atoms m^{-3}
p	Pressure	MPa
q	Inter-granular gas concentration	atoms m^{-3}
R_{ig}	Intra-granular bubble radius	m bubble^{-1}
r	Radial coordinate	m
T	Temperature	K
$t (t_{\text{irr}})$	Time (Irradiation time)	s
y	Cumulative fission yield	atoms fiss^{-1}
y_{TF}	Ternary fission yield	atoms fiss^{-1}
Z	Compressibility factor	/
γ	Intra-granular thermal re-solution rate	s^{-1}
$\lambda_{\alpha, ^{241}\text{Am}}$	Decay rate (e.g., α -decay of ^{241}Am)	s^{-1}
ρ_{fuel}	Fuel density	kg m^{-3}
$\sigma_{(n,\alpha), ^{16}\text{O}}$	Microscopic cross section (e.g., for (n, α) reaction on ^{16}O)	m^2
φ	Neutron flux	neutrons $\text{m}^{-2} \text{s}^{-1}$

2 Structure and numerical features of SCIANTIX 2.0

The current release of SCIANTIX (version 2.0) marks a significant advancement with respect to the first release of the code [32]. The code architecture has been revamped, embracing an object-oriented structure that improves overall efficiency and usability and providing a streamlined and organized structure. An intuitive and modular inclusion of several quantities relevant to the SCIANTIX simulation has been realized, representing different fuel matrices (UO_2 – generally representative for oxide fuel matrices from the IGB point of view, and UO_2 HBS – representative for the characteristics of the fuel microstructure at high burnup, or High Burnup Structure), fuel matrix properties (e.g., grain size, grain-boundary diffusivity), specific gas atoms (xenon, krypton, helium), IGB models, and numerical solvers. This modular design greatly enhances flexibility and extensibility of the code, enabling the expansion of its capabilities, e.g., by incorporating new material properties via available experimental data or atomistic/molecular dynamics simulation. Fig. 1 illustrates the flowchart of SCIANTIX. On the left side of the figure, basic features of the SCIANTIX standalone code are represented. At the beginning of the simulation, SCIANTIX elaborates the input quantities provided by the user in terms of irradiation / temperature history, initial fuel conditions and model settings. The fuel matrix, gas atoms and corresponding systems of gas atoms inside a fuel matrix are prepared. Each IGB model is constructed, including model parameters. In an independent way, numerical solvers employed by the models are declared. The separation of the SCIANTIX models from the numerical solvers allows to carry out independent verification and separate-effect validation phases.

The right side of Fig. 1 shows the SCIANTIX external driver, the latter being the external user in the code standalone version or the FPC if SCIANTIX is used as IGB module coupled to engineering-level, pin performance codes. SCIANTIX retains the same interface to preserve the coupling currently in place with FPCs (i.e., with TRANSURANUS and GERMINAL [49], [51], [53], but also OFFBEAT [31], [46] and FRAPCON/FRAPTRAN [45], [58]). Section 4 of this deliverable outlines the coupling approach of SCIANTIX with two FPCs involved in PATRICIA, i.e., TRANSURANUS and GERMINAL.

Since SCIANTIX is also designed as a module to be coupled with integral FPCs, keeping a low computational time for each simulation run / call of SCIANTIX as an FPC module is one of the goals of its development. Each SCIANTIX model includes a set of ODEs/PDEs (ordinary/partial differential equations), as described in the next Section 3. In order to limit the computational time taken by a SCIANTIX simulation, the solution of the set of the fully-coupled differential equations is approximated by using a segregated solution scheme² (or operator split approach). The differential equations considered in SCIANTIX are solved with an implicit L-stable scheme of first order, i.e., backward Euler. As a result, all numerical solutions are consistent. The numerical solvers belong to an independent class which depends only on the user input (e.g., on the choice of the specific solver, as shown in Fig. 2 where the hierarchical approach for the different code objects is illustrated) and can be recalled in the different models. Furthermore, comprehensive verification processes have been realized for each solver through the method of manufactured solution (MMS) [59], [60], and made available on the code repository [34], [35]. This verification approach allows developers of physical models to prioritize their attention on the underlying physical phenomena, disregarding errors of numerical nature.

²The operator-splitting scheme simplifies the treatment of non-linearities in state variables and model parameters, and complies with the computational time typical of a meso-scale module. Even if the operator-splitting represent a numerical approximation, experience with SCIANTIX has shown that it is suitable for IGB modelling in constant and transient conditions [8], [32], [63].

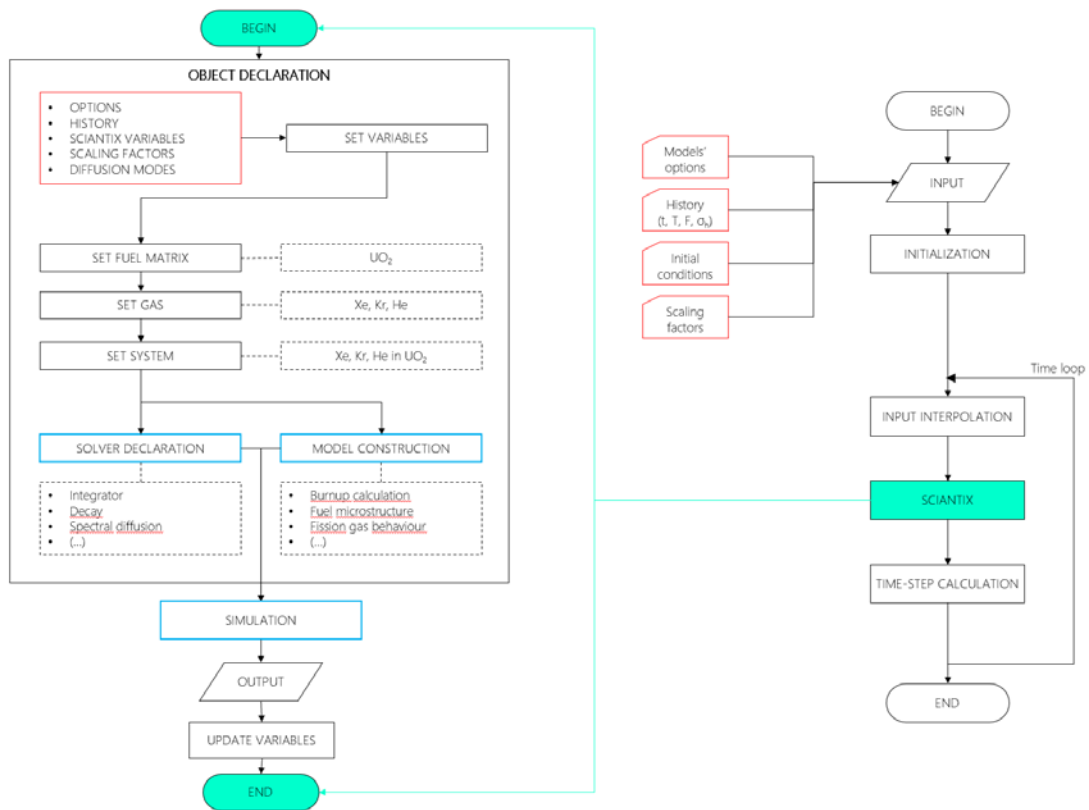


Fig. 1. Flowchart of SCIANTIX 2.0. The external driver (parent code, on the right) preserves the couplings currently in place with FPCs. The meso-scale module (for which insights are shown on the left) schematically shows how the construction of specific objects for IGB modelling is developed. It also emphasizes the logic by which the SCIANTIX simulation is obtained from the communication of specific solvers with the constructed models.

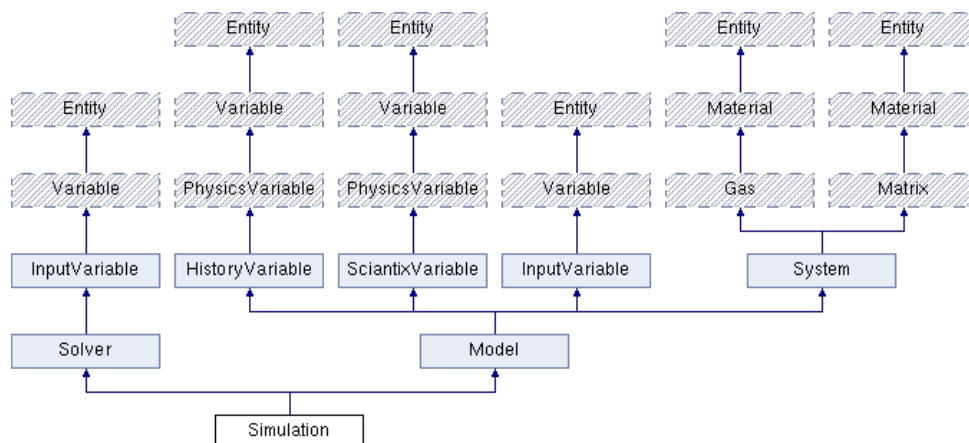


Fig. 2: Inheritance diagram (made with the Doxygen tool [61]) for the SCIANTIX simulation-object. The diagram illustrates the current internal SCIANTIX architecture and the hierarchical classification among the different sub-objects defined.

3 Inert gas behaviour modelling in SCIANTIX

The content of this Section is based on:

D. Pizzocri, M. G. Katsampiris, L. Luzzi, A. Magni, G. Zullo, *A surrogate model for the helium production rate in fast reactor MOX fuels*. Nuclear Engineering and Technology 55 (2023) 3071-3079.

L. Luzzi, A. Magni, S. Billiet, M. Di Gennaro, G. Leinders, L. G. Mariano, D. Pizzocri, M. Zanetti, G. Zullo, *Performance analysis and helium behaviour of Am-bearing fuel pins for irradiation in the MYRRHA reactor*. Submitted to Nuclear Engineering and Design, 2023.

G. Zullo, D. Pizzocri, L. Luzzi, *The SCIANTIX code for fission gas behaviour: status, upgrades, separate-effect validation, and future developments*. Submitted to Journal of Nuclear Materials, 2023.

M. Romano, D. Pizzocri, L. Luzzi, *On the intra-granular behaviour of a cocktail of inert gases in oxide nuclear fuel: Methodological recommendation for accelerated experimental investigation*. Nuclear Engineering and Technology 54 (2022) 1929-1934.

R. Giorgi, A. Cechet, L. Cognini, A. Magni, D. Pizzocri, G. Zullo, A. Schubert, P. Van Uffelen, L. Luzzi, *Physics-based modelling and validation of inter-granular helium behaviour in SCIANTIX*. Nuclear Engineering and Technology 54 (2022) 2367-2375.

D. Pizzocri, A. Cechet, L. Cognini, A. Magni, A. Schubert, P. Van Uffelen, T. Wiss, L. Luzzi, *A modelling methodology for the description of helium behaviour accounting for the grain-size distribution*. Nuclear Engineering and Design 411 (2023) 112426.

The current section describes the rate-theory models implemented in the SCIANTIX code to describe the evolution and behaviour of helium within the (oxide) nuclear fuel. The helium modelling follows the same approach adopted for fission gases (xenon and krypton) [32], [55], but considers fundamental intra- / inter-granular phenomena and peculiarities of helium behaviour that are presented in the following sub-sections. In summary, the complete chain of inter-connected processes related to fission gases (modelled in SCIANTIX) include, besides gas production in the fuel, intra-granular gas diffusion, intra-granular bubble nucleation, their growth by trapping of gas atoms and interactions of gas bubbles with high-energy fission fragments, which may result in re-resolution process for xenon and krypton (otherwise insoluble from the bubbles) back into the ceramic matrix [8]. Afterwards, the accumulation of gas in grain-face bubbles is considered, together with the phenomena of inter-granular bubble growth, interconnection by coalescence and grain-face saturation [5], [32], [62]. This description is applied to both stable fission gas isotopes (to evaluate fission gas release and gaseous fuel swelling) and radioactive fission gas isotopes (to evaluate the radioactive release from the fuel) [53], [63], [64]. Additionally, the helium behaviour description benefits from a dedicated modelling of its production (accounting in an engineering but neutronic-based way for e.g., α -decays of actinide isotopes [65], [66]) and of its diffusivity, solubility and thermal re-resolution in oxide fuel grains [10], [67], [68]. Lastly, the inert gas behaviour modelling is sided with the fuel microstructure evolution, which currently includes the evolution of the average fuel grain size [23], [55], [69], [70] and peculiar phenomena relevant for the modelling of the UO₂ high burnup structure [11], [71], [72].

In the following sub-sections, the focus is on the SCIANTIX capabilities developed during the PATRICIA Project, targeting physics-based simulations of fast reactor-type MOX fuels.

3.1 Helium production from burnup module capabilities

Besides fission gases, helium production in the nuclear fuel matrix during irradiation plays a critical role in the design and performance especially of Gen-IV reactor fuel, as it represents a life-limiting factor for the operation of fuel pins and it is relevant during fuel storage. Indeed, helium contributes to the fuel swelling and its potential release into the fuel pin free volume increases the pin internal pressure. When minor actinides (MAs, e.g., Am, Np) are included in the fuel initial composition in comparison with conventional uranium-plutonium oxide or uranium dioxide fuel, a considerable contribution to the helium production rate arises from these short-lived α -decaying nuclides. A second path to produce helium in nuclear fuel is the (n,α) reaction on ^{16}O , which is progressively more relevant under faster neutron spectra [73], [74]. The third and last path for helium production in nuclear fuel are ternary fissions, with MA isotopes having relatively higher helium yield from fast fissions compared to uranium and plutonium isotopes [75].

Depletion codes [73], [76]–[80] are the standard, high-fidelity tools applied to predict helium production following these production paths. They enable a reliable estimation of the concentration evolution of the actinides contained within the fuel by considering the sequential steady-state neutronics solution at each burnup step. Instead, fuel performance codes, dedicated to the thermo-mechanical analysis of fuel pins, typically employ less computationally expensive approaches compared to depletion codes to estimate helium production rates. These codes use either dedicated burnup modules (e.g., TUBRNP [81] employed by the FPCs TRANSURANUS [38], [39] and FRAPCON [58], or the burnup module embedded in DIONISIO [82]), directly solving the Bateman equations but with greatly simplified approaches towards cross sections³, or correlations directly calculating the helium production rate from a set of input parameters [83], [84]. These two approaches to calculate helium production have their respective advantages and disadvantages: burnup modules have greater accuracy at the expense of an increased computational cost, whereas stand-alone correlations are specific to certain fuel/reactor combinations, but fast running and inherently numerically stable.

The SCIANTIX code provides the capabilities to be exploited also as a fast-running burnup module, able to follow the inter-connected evolution during irradiation of fuel isotopes (U, Pu, MAs) and consequently to calculate the corresponding helium production. In particular, by performing multiple SCIANTIX simulations of different fuel conditions, it is possible to construct synthetic datasets on which a surrogate model for helium production is trained. The targets of this surrogate model are a computational cost comparable with that of a correlation and an accuracy in line with the requirements of engineering tools such as fuel performance codes. This methodology represents a typical application of surrogate models which is widely used in other sectors [85] and is herein proposed for fuel performance. The SCIANTIX burnup module, originally described in [86] and firstly showcased for U-Pu MOX fuels, is extended to wider ranges of U-Pu MOX and to Am-MOX fuels leveraging high-fidelity results from the SERPENT Monte Carlo code [87], [88] to generate macroscopic cross-section lookup tables specific for fuel/reactor combinations. The extended burnup module is then used to generate synthetic datasets covering a wide range of initial fuel compositions and irradiation conditions, and a surrogate model for the helium production rate is developed based on non-linear multivariate regression performed on the datasets.

On the basis of the actinide nuclides that SCIANTIX currently considers [86], the resulting Bateman equation for the helium production rate in the SCIANTIX burnup module is:

³ Typical hypotheses are (i) considering burnup-averaged cross section values assessed based on *a priori* estimation of fuel composition evolution, and (ii) considering one energy group of neutrons. The resulting average cross section values are typically adjusted to match validation results, which results in burnup modules of FPCs being fast running and reliable besides being based on strong assumptions.

$$\begin{aligned}
\frac{d[{}^4\text{He}]}{dt} = & \lambda_{\alpha,234\text{U}} [{}^{234}\text{U}] + \lambda_{\alpha,235\text{U}} [{}^{235}\text{U}] + \lambda_{\alpha,236\text{U}} [{}^{236}\text{U}] + \lambda_{\alpha,238\text{U}} [{}^{238}\text{U}] \\
& + \lambda_{\alpha,237\text{Np}} [{}^{237}\text{Np}] \\
& + \lambda_{\alpha,238\text{Pu}} [{}^{238}\text{Pu}] + \lambda_{\alpha,239\text{Pu}} [{}^{239}\text{Pu}] + \lambda_{\alpha,240\text{Pu}} [{}^{240}\text{Pu}] + \lambda_{\alpha,242\text{Pu}} [{}^{242}\text{Pu}] \\
& + \lambda_{\alpha,241\text{Am}} [{}^{241}\text{Am}] + \lambda_{\alpha,243\text{Am}} [{}^{243}\text{Am}] \\
& + \lambda_{\alpha,242\text{Cm}} [{}^{242}\text{Cm}] + \lambda_{\alpha,243\text{Cm}} [{}^{243}\text{Cm}] + \lambda_{\alpha,244\text{Cm}} [{}^{244}\text{Cm}] + \lambda_{\alpha,245\text{Cm}} [{}^{245}\text{Cm}] \\
& + \sigma_{(n,\alpha),{}^{16}\text{O}} \varphi [{}^{16}\text{O}] \\
& + y_{TF} \dot{F}
\end{aligned} \tag{1}$$

where $[X]$ (at m^{-3}) is the concentration of the nuclide iX , $\lambda_{\alpha, iX}$ (s^{-1}) is the α -decay constant of the nuclide iX , $\sigma_{(n,\alpha),{}^{16}\text{O}}$ (m^2) is the (n,α) reaction cross-section of ${}^{16}\text{O}$, φ (neutrons $\text{m}^{-2} \text{s}^{-1}$) is the local neutron flux ⁴, y_{TF} is the ternary fission yield which is equal to 0.22% [89], and \dot{F} (fissions $\text{m}^{-3} \text{s}^{-1}$) is the local fission rate density. At each time step, a two-step procedure is performed: (1) the cross-section values for each nuclear reaction type regarding all nuclides are calculated from lookup tables based on the local burnup and initial fuel composition via an interpolation algorithm, and (2) the numerical integration of the Bateman equations, covering actinide isotopes and including helium - Eq. (1), is performed via a first order implicit numerical scheme.

The following sub-sections are dedicated to the methodology followed to develop and extend the SCIANITX burnup module capabilities and to build surrogate models for helium production (Section 3.1.1), which are then presented and assessed. In particular, Section 3.1.2 is dedicated to He production in generic fast reactor cases (SFR – sodium-cooled fast reactor, and LBE-FR – lead-bismuth eutectic fast reactor) [65], while Section 3.1.3 focuses on the MYRRHA “Revision 1.8” irradiation conditions [66], [90].

3.1.1 Methodology

The methodology used to extend the SCIANITX burnup module [65] follows a standardized development procedure for the module that was originally designed as [86]:

1. A set of high-fidelity SERPENT simulations is performed for an initial fuel composition vector, corresponding to the fuel/reactor combination under evaluation.
2. For each initial composition step e_i and each burnup step bu_i , the respective cross-section values are extracted, evaluated by the reaction rate integrals in the SERPENT simulation.
3. A $(e_i \times bu_i)$ matrix is created containing the microscopic cross-section values, with each row representing the initial enrichment steps and each column the burnup steps for each nuclide and each reaction type.
4. These matrices are implemented in the burnup module routines of the SCIANITX code as lookup tables corresponding to the fuel/reactor combinations of interest.

The domain of the SERPENT simulations performed in this work consists of a single fuel pin with cylindrical geometry, composed of the uniform fuel pellet, the fuel-cladding gap and the cladding, encompassed by the coolant material. The simulation universe is a cube of side length equal to the fuel pin length. A reflective boundary condition is applied at the end-surfaces of the defined simulation

⁴ The local neutron flux is calculated by $\varphi = \dot{F} / \overline{\Sigma}_f$ where $\overline{\Sigma}_f$ (m^{-1}) is the approximated one-group macroscopic fission cross-section calculated over m -fissile nuclides as $\overline{\Sigma}_f = \sum_m \overline{\sigma}_{f,mX} [{}^mX]$, where $\overline{\sigma}_{f,mX}$ (m^2) is the microscopic fission cross-section of nuclide mX .

universe [87]. The SERPENT package used, for all the simulation cases herein considered, contains libraries based on JEF-2.2, JEFF-3.1, ENDF/B-VI.8 and ENDF/B-VII evaluated data files [65]. Subsequently, the extended lookup tables of cross sections obtained from SERPENT results are implemented in the SCIANTIX burnup module routines.

The SCIANTIX burnup module interpolates cross-sections from lookup tables constructed from high-fidelity depletion calculations. These rely on SERPENT for the evaluation of the reaction rate integrals in the fuel. To obtain the absolute value of the reaction rate integrals, SERPENT considers a user-defined source normalization term. The SERPENT depletion calculation adopts the Chebyshev Rational Approximation Method (CRAM) used for the decomposition and solution of the system determined by the burnup matrix. A predictor-corrector algorithm is used for each calculation node, with linear extrapolation occurring in the predictor step for time integration and linear interpolation occurring in the corrector step. An initial neutron population of 10^4 neutrons is used, with 100 active and 30 inactive cycles, which facilitates reasonable computational times associated to a relatively low standard deviation.

The outlined methodology is used to populate several synthetic datasets of calculated helium concentration values as a function of the input variable matrix. The output vector $Y_{N,n}$ (i.e., the helium concentration produced under certain fuel conditions) is calculated by the code as a function of a selection of n values of N input variables composing the input matrix $I_{N,n}$, sampled from pre-defined ranges. By examining the probability distribution of the output $Y_{N,n}(I_{N,n})$ the desired information of the dependence of the helium concentration on each input variable can be obtained. The number of input variables N and the number of values sampled n dictate the computational time for the creation of the synthetic datasets (e.g., for the generation of a dataset of 10000 values, the computational time required is around three hours).

To ensure that the entire distribution of each of the input variables $I_{i,n}$ is represented by the input values sampled, the Latin Hypercube Sampling (LHS) technique is adopted: the range of each $I_{i,n}$ is divided into M strata of equal marginal probability $1/M$ and sampled only once from each stratum [91]. This technique brings the advantage of limiting the amount of input values per each input variable and representing them in a fully stratified manner, without a biased projection of the values that ends up being important in the final model from a statistical point of view. As an example, the Pu/HM (Heavy Metal) input variable distribution for 881 data points is provided in [65] and corresponds to a dense coverage of values over the sampling space.

The input variables considered in this work are the fuel initial fuel composition in terms of all constituent nuclides expressed as the ratio of each nuclide per heavy metal (iX/HM), the initial oxygen to metal ratio (O/M) of the fuel, the initial fuel density ρ_{fuel} , the fuel (local) temperature T_{fuel} , the irradiation time t_{irr} and the fission rate density \dot{F} . The sampling ranges of each variable are chosen in line with the predictive capabilities of the extended SCIANTIX burnup module as well as with the fuel specifications of a selection of Generation IV reactor core concepts [92]. The implementation of the LHS technique is performed in MATLAB [93] coupled with the SCIANTIX code for the helium concentration calculations. The training dataset is composed of the multidimensional input matrix $I_{N,n}$ representing the contribution of each input variable, together with the output vector $Y_{N,n}$. Subsequently, multivariate non-linear regression and statistical analysis are performed to formulate a final model for a certain fuel/reactor combinations of interest. The method of stepwise regression employed is forward regression.

The regression is performed by accounting for the p -values of each regressor with respect to the output values in an iterative process, in which each regressor is added to the model formulation on the basis of its p -value (on the training dataset considered) being below the 0.05 threshold, i.e., a 95% of confidence on the significance of that regressor. Within this approach, collinearity between input variables is

avoided by including only one of the inter-correlated variables in the final model (e.g., irradiation time and fission rate density are heavily correlated with burnup, thus the latter is excluded from the final model, given also that the former two variables are directly used as inputs of the SCIANTIX burnup module). At each iteration step, after a variable has been added to the model, the *p-values* are re-evaluated since they change accordingly for each regressor.

Schemes of the standardized methodology applied for the generation of the cross-section lookup tables for any fuel/reactor combination and of the process of developing a surrogate model for the helium production rate are provided in Figs. 3 and 4.

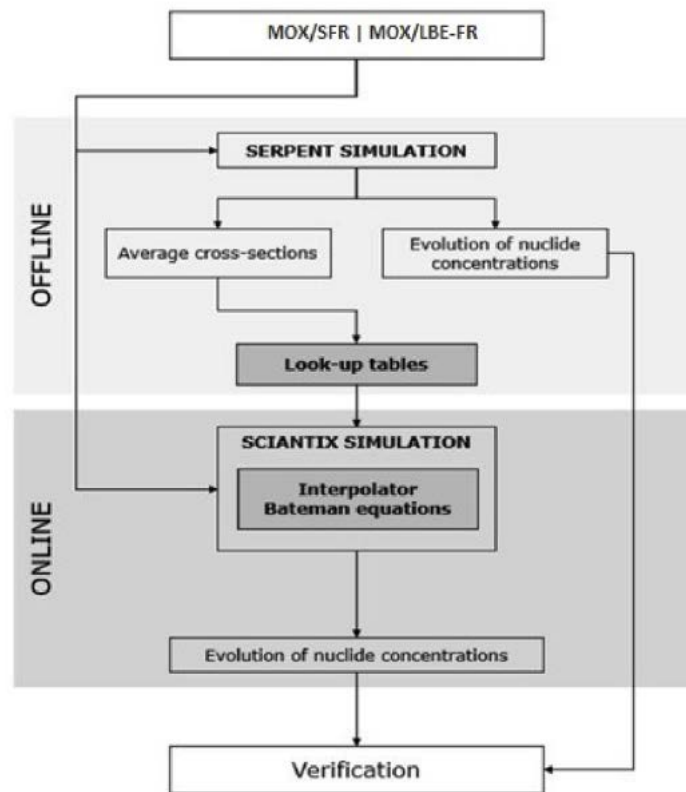


Fig. 3. Standardized methodology applied for the generation of the cross-section lookup tables for the corresponding fuel/reactor combination. SERPENT simulations are performed OFFLINE, while the SCIANTIX simulations are performed ONLINE.

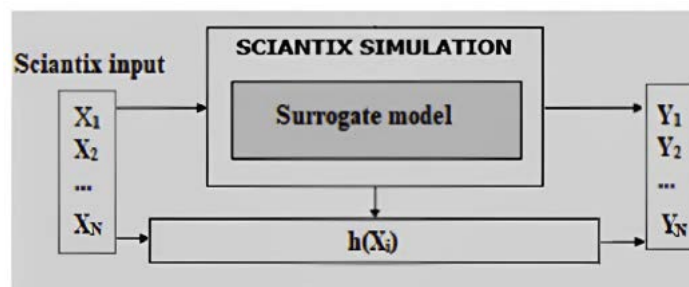


Fig. 4. Schematic representation of the process of developing a surrogate model for the helium production rate. First, SCIANTIX burnup module is used to obtain a dataset relating the output vector to the input matrix. Secondly, the surrogate model $h(X_i)$ is developed based on the training dataset.

3.1.2 Surrogate model for fast reactor conditions

Two fast reactor cases are first targeted, i.e., a sodium cooled fast reactor (SFR) and a lead-bismuth eutectic-cooled fast reactor (LBE-FR).

The specifications of the SERPENT simulation are collected in Tab. 2. The high-fidelity depletion calculation was performed in 81 burnup steps, equally distanced of 2.5 GWd/t_{HM} from 0 up to 200 GWd/t_{HM}, and 31 plutonium enrichment (Pu/HM) steps starting from 20 up to 51 at.%. A reactor power of 40 kW kg⁻¹ has been assumed [86], corresponding to a fission rate density of 1.32 10¹⁹ fissions m⁻³ s⁻¹ for the SFR case and of 1.17 10¹⁹ fissions m⁻³ s⁻¹ for the LBE-FR case, with a fission energy of 3.33 10⁻¹³ J (208 MeV). Cross section values are calculated by SERPENT at each node of the (burnup x enrichment) matrix, as well as away from these points, according to an area-weighted procedure explained in [86]. These output data from SERPENT compose the SCIANTIX lookup tables, as outlined in the previous Section 3.1.1.

Tab. 3 collects the settings of the sets of SCIANTIX simulations performed for the two FR irradiation cases under consideration. First, the predictive capabilities of the extended SCIANTIX burnup module in both simulation cases are verified against the high-fidelity SERPENT results. The verification is performed for the 31 initial fuel enrichment steps, for each of the nuclides considered by the burnup module [86]. The average RMSE (Root-Mean-Square Error) for all the plutonium enrichment steps considered is shown in Fig. 5, where it is evident that the extended burnup module has a consistently better predictive performance compared to the previous version [86]. The gain in RMSE is limited for initial Pu enrichments up to 41 at.%, while it improves significantly at higher fuel Pu contents.

Table 2. Specifications of the SERPENT simulations for the two fuel/reactor combinations.

Parameter	MOX/SFR	MOX/LBE-FR
External pellet radius (mm)	2.71	2.71
Radial gap (mm)	0.116	0.116
U/HM (%)	80-49 ^a	80-49 ^a
Pu/HM (%)	20-51 ^b	20-51 ^b
Enrichment step width (at/HM.%)	1	1
O/M ratio	1.957	1.957
Fuel density (kg m ⁻³)	10970	10970
Column length (mm)	850	850
Cladding material	15-15 Ti-stabilized SS ^c	15-15 Ti-stabilized SS ^c
Cladding thickness	0.45	0.45
Cladding density (kg m ⁻³)	7950	7950
Coolant	Sodium	Lead-Bismuth Eutectic (Pb 45 wt.%, Bi 55 wt.%)
Simulation universe side length(mm)	870	870
Coolant density (kg m ⁻³)	610	10280
Total burnup (GWd t _{HM} ⁻¹)	200	200
Burnup step width (GWd/t _{HM})	2.5	2.5
Burnup steps	81	81
Fission rate density (m ⁻³ s ⁻¹)	1.32 · 10 ¹⁹	1.17 · 10 ¹⁹

^a Natural uranium composition

^b ²³⁸Pu 1.3 wt.%, ²³⁹Pu 60.4 wt.%, ²⁴⁰Pu 23.4 wt.%, ²⁴¹Pu 10.4 wt.%, ²⁴²Pu 4.5 wt.%.
^c C 0.01 wt.%, Ca < 0.01 wt.%, Co < 0.03 wt.%, Cr 15.1 wt.%, Cu < 0.05 wt.%, Mn < 2 wt.%, Mo 1.2 wt.%, N < 0.015 wt.%, Ni 15 wt.%, P < 0.015 wt.%, Si 0.4 wt.%, Ti 0.5 wt.%

Table 3. Specifications of the SCIANTIX simulations for the two fuel/reactor combinations.

Parameter	MOX/SFR	MOX/LBE-FR
Number of history points	81	81
Number of time steps per history point	1000	1000
Irradiation time (h)	120000	106000
Burn-up at discharge (GWd t _{HM} ⁻¹)	226	200
Fission rate density (fissions m ⁻³ s ⁻¹)	1.32 · 10 ¹⁹	1.17 · 10 ¹⁹
Fuel density (kg m ⁻³)	10970	10970
O/M ratio	1.957	1.957

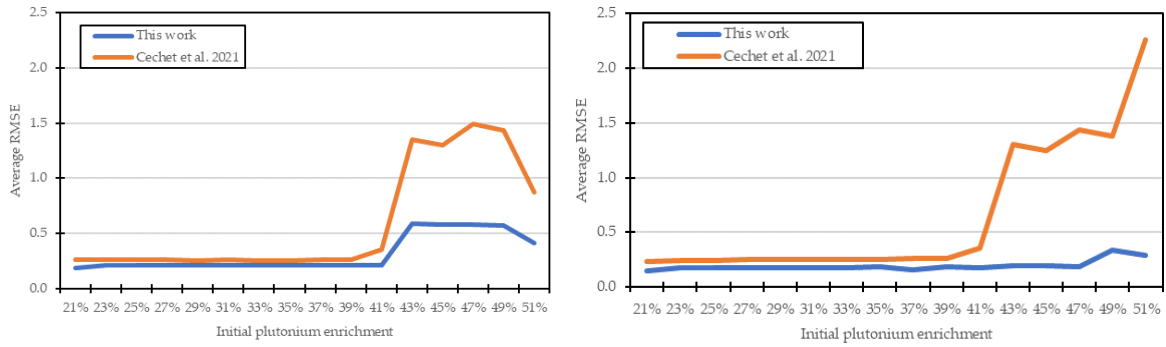


Fig. 5. Comparison of the RMSE (averaged in burnup and on all nuclides) between the SCIANTIX burnup module and SERPENT reference results for the SFR case (left) and for the LBE-FR case (right), as a function of initial plutonium enrichment of the fuel.

The construction of surrogate models representative of the He production in the fuel/reactor combinations considered, i.e., the SFR and LBE-FR irradiation cases, starts from the consideration of the input variables ranges collected in Tab. 4. After an analysis of the sensitivity of the helium production to each of those input variables and of the statistics (e.g., *p-values*) associated to each regressor, the surrogate models (one for each irradiation case) include seven dependencies:

- Irradiation time t_{irr} (h)
- Fission rate density \dot{F} (fissions $\text{m}^{-3} \text{s}^{-1}$)
- Total plutonium content Pu/HM (at.%)
- Fuel density ρ_{fuel} (kg m^{-3})
- Initial americium-241 concentration $^{241}\text{Am}/\text{HM}$ (at.%)
- Initial americium-242 concentration $^{242}\text{Am}/\text{HM}$ (at.%)
- Initial curium-242 concentration $^{242}\text{Cm}/\text{HM}$ (at.%)

The quality of the final fit and the accuracy of the models were quantified in terms of the RMSE, the coefficient of determination R^2 and the adjusted coefficient of determination R^2_{adj} [94]. The proposed surrogate models for the SFR and the LBE-FR cases are both in the form:

$$\frac{d[{}^4\text{He}]}{dt_{\text{irr}}} = A t_{\text{irr}}^{A-1} 10^P, \quad (2)$$

$$P = B \dot{F} + (C [\text{Pu}] + D [\text{Pu}]^2 + E [\text{Pu}]^3) + F \rho_{\text{fuel}} + G [{}^{241}\text{Am}] + H [{}^{242}\text{Am}] + I [{}^{242}\text{Cm}] + S$$

where A , B , C , D , E , F , G , H , I and S are coefficients, reported in Tab. 5, for the two fuel/reactor combination cases along with the respective standard errors. An in-depth look at coefficient values indicates minor differences between the SFR and LBE-FR cases considered: the values and the relative weights of the coefficients in the two surrogate models are similar, indicating that the dominant paths of helium production are comparable in these two reactor/fuel concepts, as expected from the similar fuel and cladding compositions reported in Tab. 2.

Eq. (2) can be analytically solved for $\text{Log}[{}^4\text{He}]$. The functional dependencies on the parameters are not representative of a physical behaviour but are the results of a data-driven selection among possible dependencies and are valid within the ranges reported in Tab. 4. The statistical method used to produce the functional form of Eq. (2) is akin to a machine learning approach, in the sense that it links inputs and outputs in a significant way without the need to incorporate an *a priori* physical description.

Since the proposed surrogate model is made of a single ordinary differential equation, its computational requirement is significantly reduced compared to the use of state-of-the-art burnup modules adopted in fuel performance codes, which require the coupled solution of tens to hundreds of ordinary differential equations.

Table 4. Ranges of the input variable values considered for the development of the surrogate model for helium production in the SFR and LBE-FR cases.

Variable	Symbol	Range
Irradiation time (h)	t_{irr}	100 – 100000
O/M (/)	O/M	1.95 – 2.00
Fission rate density (fissions $m^{-3} s^{-1}$)	\dot{F}	$1 \cdot 10^{18} - 1 \cdot 10^{19}$
^{235}U enrichment (at.%)	[^{235}U]	0.711 – 5
Pu/HM (at.%)	[Pu]	20 – 50
Np/HM (at.%)	[Np]	0 – 5
Am/HM (at.%)	[Am]	0 – 5
Cm/HM (at.%)	[Cm]	0 – 5
Fuel density ($kg m^{-3}$)	ρ_{fuel}	9325 – 10970
Fuel temperature (K)	T_{fuel}	900 – 1900

Table 5. Values of the coefficients in the surrogate model for the helium production rate for the two fuel/reactor combinations, with the corresponding standard error.

Coefficient	Variable	Estimate (SFR case)	Standard error	Estimate (LBE-FR case)	Standard error
<i>A</i>	t_{irr}	$6.70 \cdot 10^{-1}$	$3.84 \cdot 10^{-3}$	$6.77 \cdot 10^{-1}$	$3.75 \cdot 10^{-3}$
<i>B</i>	\dot{F}	$2.58 \cdot 10^{-21}$	$6.05 \cdot 10^{-23}$	$2.66 \cdot 10^{-21}$	$5.87 \cdot 10^{-23}$
<i>C</i>	[Pu]	$-9.01 \cdot 10^{-1}$	$1.36 \cdot 10^{-2}$	$-9.25 \cdot 10^{-1}$	$1.31 \cdot 10^{-2}$
<i>D</i>	[Pu] ²	$2.38 \cdot 10^{-2}$	$3.91 \cdot 10^{-4}$	$2.44 \cdot 10^{-2}$	$3.77 \cdot 10^{-4}$
<i>E</i>	[Pu] ³	$-2.05 \cdot 10^{-4}$	$3.65 \cdot 10^{-6}$	$-2.10 \cdot 10^{-4}$	$3.51 \cdot 10^{-6}$
<i>F</i>	ρ_{fuel}	$3.12 \cdot 10^{-5}$	$3.49 \cdot 10^{-6}$	$3.75 \cdot 10^{-5}$	$3.38 \cdot 10^{-6}$
<i>G</i>	[^{241}Am]	$6.80 \cdot 10^{-2}$	$3.99 \cdot 10^{-3}$	$7.37 \cdot 10^{-2}$	$3.78 \cdot 10^{-3}$
<i>H</i>	[^{242}Am]	$1.69 \cdot 10^{-1}$	$3.97 \cdot 10^{-3}$	$1.61 \cdot 10^{-1}$	$3.87 \cdot 10^{-3}$
<i>I</i>	[^{242}Cm]	$1.85 \cdot 10^{-1}$	$3.05 \cdot 10^{-3}$	$1.79 \cdot 10^{-1}$	$2.98 \cdot 10^{-3}$
<i>S</i>	-	34.1	$1.58 \cdot 10^{-1}$	34.3	$1.51 \cdot 10^{-1}$

For the development of the two surrogate models, two training datasets were generated using the LHS method to feed the extended SCIANITX burnup module, as discussed in Section 3.1.1. The training dataset for the SFR case is composed of $n = 8538$ data points, while that for the LBE-FR case of $n = 8579$ data points. Apart from these two training datasets, independent validation datasets are generated for both simulation cases, with different sizes and variable limits, to assess the predictive capability of the proposed surrogate models in a variety of different conditions. The details of each validation dataset are reported in [65] and in Tab. 6 for the LBE-FR case. Generally, they reflect possible applicative cases for

the surrogate models, targeting the specifications and irradiation conditions of relevant fast reactor concepts.

The validation of the performance of the surrogate model for He production in the LBE-FR case is discussed here (Fig. 6). As expected, it exhibits the best performance for the training dataset, but the predictive capability is as well satisfactory against the validation datasets, particularly considering the wide applicability range in terms of irradiation conditions. Most of the points of the clouds in Fig. 6 are concentrated around the plot diagonal, meaning the perfect agreement between data and calculations. The RMSE ranges from around 0.15 to 0.31, and the R^2 and R^2_{adj} statistic metrics range from around 0.51 to 0.84, indicating a reasonable fit of the surrogate model to the values produced from the extended SCIANTIX burnup module. The variance associated with the predicted values occurs due to the high number of input variable combinations (namely, irradiation time and fission rate density) which lead to different burnup values for each initial fuel composition. Moreover, from the statistical analysis performed on the surrogate model, the burnup turned out to be the strongest parameter that affects helium production in the analyzed conditions. As a general tendency, with a higher number of data points in the dataset, a better agreement is observed as a denser matrix of input values is generated.

Table 6. Datasets generated with the extended SCIANTIX burnup module and used for training and validation of the surrogate model for the helium production rate (LBE-FR case).

Dataset	Number of data points, n	Specifications
Training	8579	Full variable ranges
Validation	84648	Am/HM = 0
Validation	9968	Constant Pu/HM = 20%
Validation	313	Constant Pu/HM = 50%

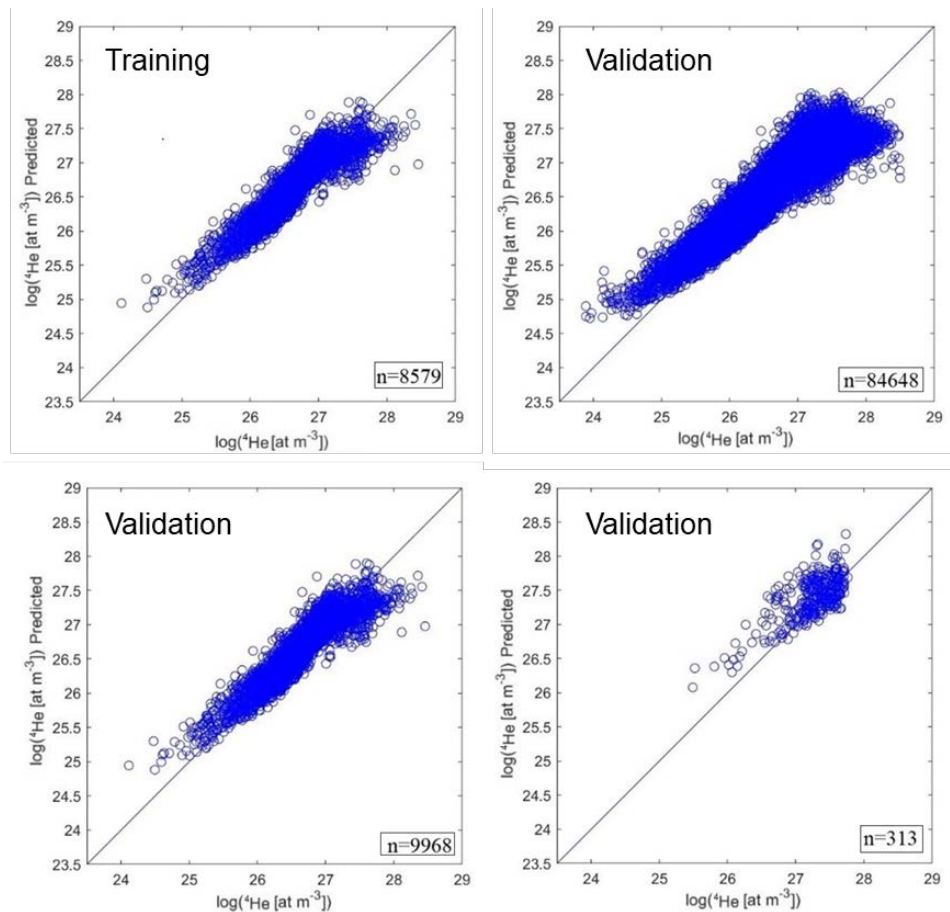


Fig. 6. Evaluation of the proposed surrogate model for the helium production rate (y-axis) against the values calculated by the SCIANTIX burnup module (x-axis) for four datasets representative of the LBE-FR case, where (top-left) is the training dataset while the others are validation datasets.

3.1.3 Surrogate model for MYRRHA irradiation conditions

The same methodology outlined in Section 3.1.1 is also applied to derive a surrogate model of helium production in Am-MOX fuels under MYRRHA irradiation conditions, referring to the MYRRHA core design “Revision 1.8” (sub-critical, accelerator-driven) of reference within the PATRICIA Project [90]. This development benefits from the extension of the SCIANTIX burnup module targeting FR-type Am-MOX already performed in [65] (Section 3.1.2). The present modelling activity focuses on a specific irradiation position within the MYRRHA core, i.e., the In-Pile test Section (IPS), to be exploited for irradiation experiments on Am-MOX fuel pins. Despite this, the ranges of validity of the developed He production model are wide enough to generally cover the irradiation conditions of MYRRHA driver fuel, from the first loading in the first core ring (the closest to the central spallation target) up to the last irradiation cycle at the core periphery before fuel discharge [66], [90]. Moreover, the resulting model provides the explicit dependency on the fuel Am content (similarly to Section 3.1.2), hence enabling to account for this relevant effect on the He production in a reliable but engineering way, and to isolate it for dedicated uncertainty and sensitivity analysis.

For what concerns the cross-section derivation from the SERPENT offline step, one important aspect to be considered is that SERPENT cannot simulate spallation reactions, hence the high-energy contribution to the MYRRHA neutron spectrum (Fig. 7) provided by the external accelerator coupled to the reactor core in the sub-critical, accelerator-driven configuration. In principle, this high-energy “shoulder” of the

spectrum impacts both the Am evolution and He production under irradiation. Nevertheless, relying on a critical core SERPENT model to estimate the macroscopic cross sections for the burnup calculations is still a reasonable approximation if the high-energy region of the spectrum (> 20 MeV) is small compared to the < 20 MeV part, and the cross sections values at high energies do not increase significantly. In this scenario, the spallation spectrum has a low weight in the cross section calculation process. Both the aforementioned conditions are satisfied in the MYRRHA case: (i) in the second ring of the MYRRHA core where the IPS position is placed, the > 20 MeV flux is less than 1% of the local fast flux (at energies > 0.1 MeV). This fraction decreases towards the core periphery, i.e., the farther the position is from the core central spallation target [90] (ii) the fission cross sections generally increase between 0.1 and 1 MeV and then the values keep nearly constant at energies > 1 MeV [95], [96]. This justifies the validity of the SERPENT modelling and calculation as a first step of the methodology applied to MYRRHA.

The comparison between the actual MYRRHA neutron spectrum as a function of energy (in the MYRRHA-IPS irradiation position, for the reference composition of Am-MOX considered, i.e., containing 0.49 wt.% of Am-241) and the spectrum derived from the SERPENT step of the burnup module methodology is provided in Fig. 7. Moreover, the geometry employed for the SERPENT calculations on MYRRHA is an infinite hexagonal lattice with the same dimensions (e.g., radius, pin pitch, active length) as in the MYRRHA current design [66], [90], as well as the same cladding and coolant compositions, while no structural materials are included in the SERPENT model.

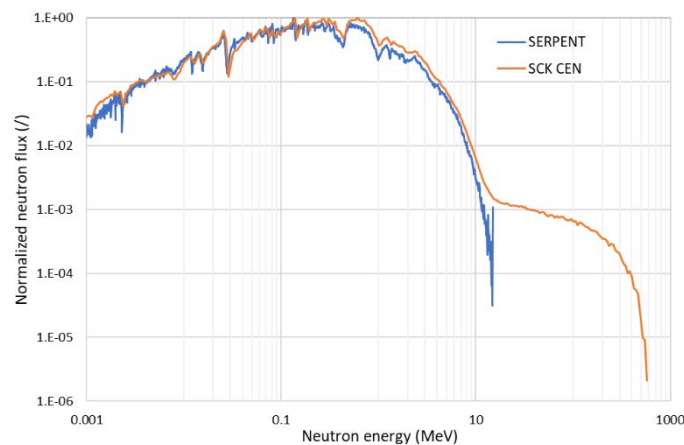


Fig. 7. Normalized neutron spectrum in the MYRRHA IPS channel (obtained by neutronic simulations performed at SCK CEN for the 0.49 wt.% Am fuel content [90]) compared to the one derived from the SERPENT offline step and employed in this work for the application of the SCIANTIX burnup module methodology to MYRRHA “Revision 1.8”. The spectrum is here shown for energies > 1 keV (where the neutron flux is more than 1% of its maximum value per energy bin) and includes the high-energy spallation contribution for energies > 10 MeV.

The results of the SCIANTIX burnup module on the MYRRHA Am-MOX (at the reference Am content of 0.49 wt.% and at 5 wt.% Am), working with cross sections customized for the MYRRHA reactor, are verified against the results of the SERPENT simulations and of TUBRNP (the TRANSURANUS burnup module [81], [97]) under the same conditions, i.e., a continuous irradiation at the IPS neutron flux level up to an extended burnup of 200 GWd/ t_{HM} . Fig. 8 shows the evolution of three nuclides which are particularly significant for the helium production in Am-MOX fuels, besides the helium production itself. The SCIANTIX burnup module, besides allowing the use of cross sections specific for the MYRRHA conditions, enables an advanced description of the He production evolution with burnup since it considers (in line with the SERPENT high-fidelity calculations) more α -emitting nuclides than TUBRNP. It should be recalled that TUBRNP is currently verified up to 100 GWd/ t_{HM} , so its predictions are herein extrapolated out of range towards very high burnup levels [81].

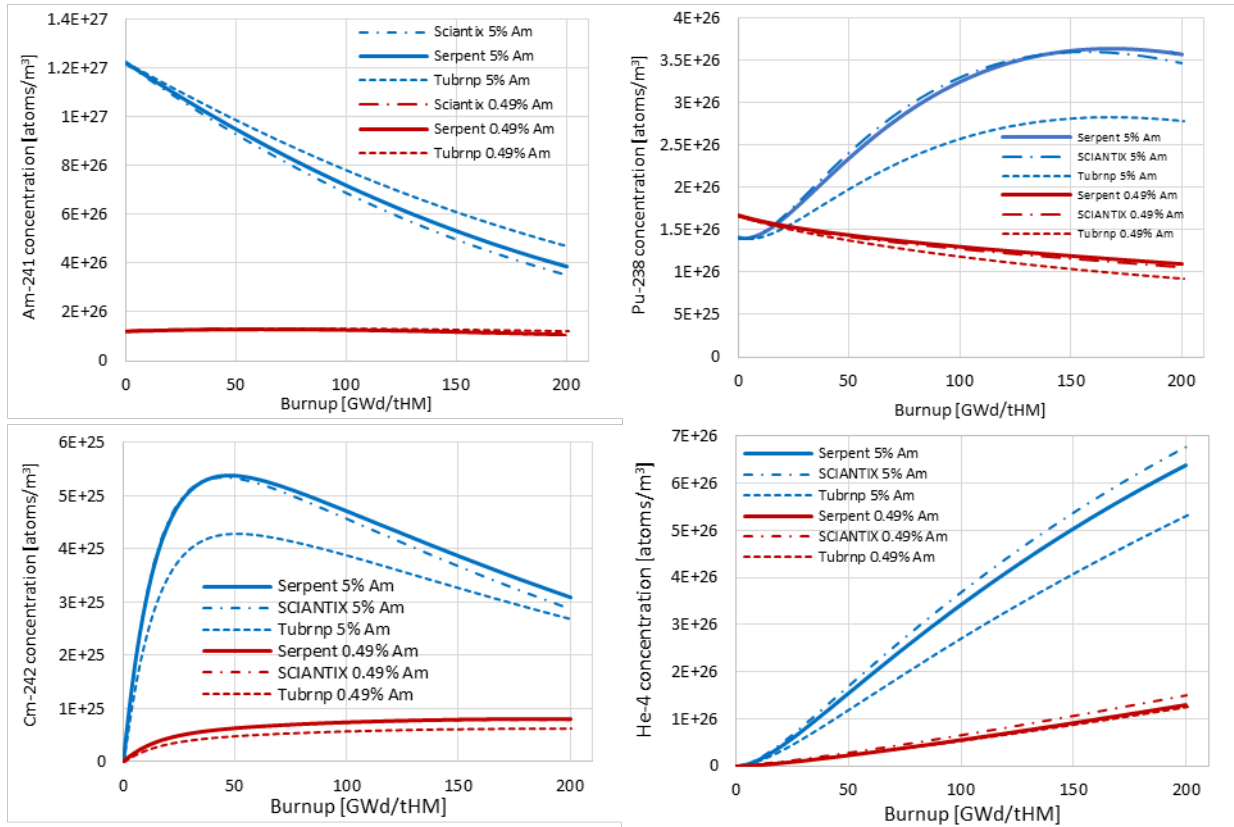


Fig. 8. Evolution of the average concentration of different nuclides at two different americium loadings, in terms of average fuel burnup, computed with TUBRNP (which is verified up to 100 GWd_{th}/t_{HM} [81], [86]), the SCIANITX burnup module extended to Am-bearing fuels and the high-fidelity SERPENT simulation (MYRRHA-IPS irradiation conditions).

Based on the results of the SCIANITX burnup module for helium production in the MYRRHA-IPS scenario, a surrogate model is developed to describe the He production rate for the Am-MOX fuel under both IPS and driver-fuel MYRRHA irradiation conditions. The main aim is to achieve a description capable of accounting for the actual irradiation conditions and fuel composition during the MYRRHA irradiation. Additionally, as for the models developed in Section 3.1.2, this surrogate model allows fast computational times, suitable for implementation in / coupling with fuel performance codes, compared to the running times of burnup modules [86]. The model derivation is performed by best-fitting the synthetic dataset of He production values provided by SCIANITX, in wide ranges of irradiation conditions and fuel compositions (Tab. 7). Similarly to Section 3.1.2, statistical analyses on the p-values associated to each model regressor are again performed, to assess the significance of the proposed model formulation against the fitted data. The resulting surrogate model for the He production rate, which proved to best represent the synthetic “training” dataset derived via multiple SCIANITX simulations, reads:

$$\frac{d[{}^4\text{He}]}{dt} = \left(A [{}^{241}\text{Am}] + B [{}^{241}\text{Am}]^2 + C \right) + 2 t_{\text{irr}} \left(D [{}^{241}\text{Am}] + E [{}^{241}\text{Am}]^2 + F \right) + \quad (3)$$

$$F (G [^{241}\text{Am}] + H) + 2 t_{irr} (\dot{F})^2 (I [^{241}\text{Am}] + J) - K [^{241}\text{Am}] \frac{\dot{F}}{X} \left(\frac{t_{irr} \dot{F}}{X} - 1 \right) e^{-\left(\frac{t_{irr} \dot{F}}{X} \right)}$$

where the coefficient values are listed in Tab. 8 and hold for Am concentration $[^{241}\text{Am}]$ expressed in wt.%, irradiation time t_{irr} in hours, and fission rate density \dot{F} in fissions $\text{m}^{-3} \text{s}^{-1}$. This model can replicate with great accuracy the results of helium production from the SCIANTIX burnup module within the validity intervals (Tab. 7), i.e., the model verification against training dataset is confirmed, as shown in Fig. 9 - left. It is also successfully validated against additional, independent datasets for which the input parameters have been sampled randomly within the same ranges of values (Tab. 7), as shown in Fig. 9 – right. The proposed model shows robustness also outside of its validity intervals, e.g., against datasets corresponding to up to 10 wt.% of Am, lower fission rate densities down to $0.9 \cdot 10^{19}$ fissions $\text{m}^{-3} \text{s}^{-1}$ or up to $3.0 \cdot 10^{19}$ fissions $\text{m}^{-3} \text{s}^{-1}$, hence covering the whole range of irradiation conditions designed for the driver fuel (i.e., the entire pin irradiation history from cycle 1 to cycle 13) in MYRRHA “Revision 1.8”. The RMSEs associated to these additional datasets are: 0.07 for the “validation” dataset of Fig. 9 – right, 0.49 for the dataset up to 10 wt.% of Am content in the fuel, 0.22 and 0.12 for the “lower power” and “higher power” datasets, respectively.

Table 7. Ranges of irradiation data used for the SCIANTIX burnup module simulations, equipped with specific cross section tables, to produce synthetic datasets of helium production in the MYRRHA Am-MOX fuel (MYRRHA-IPS irradiation conditions).

Variable	Range
Fission rate density [fissions $\text{m}^{-3} \text{s}^{-1}$]	$[(1.3 \div 2.3) \cdot 10^{19}]^a$
Burnup [GWd t_{HM}^{-1}]	$[0 \div 200]$
Am concentration [wt.%]	$[0 \div 5]$
Pu concentration [wt.%]	$[30 \div 25] (30 - \text{Am})$
U-235 enrichment / U [wt.%]	0.711
O/M as-fabricated [-]	1.969
Temperature [°C]	$[550 \div 1200]^a$

^a The fission rate interval corresponds to the values of the IPS fuel pin at different axial positions. The temperature range covers the values experienced by the fuel during the IPS irradiation (outer temperature ÷ inner temperature) at different Am contents in the range $[0 \div 5]$ wt.%.

Table 8. Coefficient values and associated standard errors of the proposed model for helium production in the MYRRHA Am-MOX fuel.

Coefficient	Estimate	Standard error
<i>A</i>	$3.387 \cdot 10^{20}$	$2.145 \cdot 10^{18}$
<i>B</i>	$2.717 \cdot 10^{19}$	$2.057 \cdot 10^{17}$
<i>C</i>	$3.528 \cdot 10^{20}$	$5.560 \cdot 10^{18}$
<i>D</i>	$- 9.692 \cdot 10^{14}$	$1.991 \cdot 10^{13}$
<i>E</i>	$- 2.397 \cdot 10^{14}$	$2.880 \cdot 10^{12}$
<i>F</i>	$2.057 \cdot 10^{15}$	$4.176 \cdot 10^{13}$
<i>G</i>	80.77	$1.146 \cdot 10^{-1}$
<i>H</i>	8.864	$3.263 \cdot 10^{-1}$
<i>I</i>	$- 1.252 \cdot 10^{-23}$	$5.411 \cdot 10^{-26}$
<i>J</i>	$1.811 \cdot 10^{-23}$	$1.480 \cdot 10^{-25}$
<i>K</i>	$- 1.970 \cdot 10^{25}$	$1.971 \cdot 10^{22}$
<i>X</i>	$2.218 \cdot 10^{23}$	$3.218 \cdot 10^{20}$

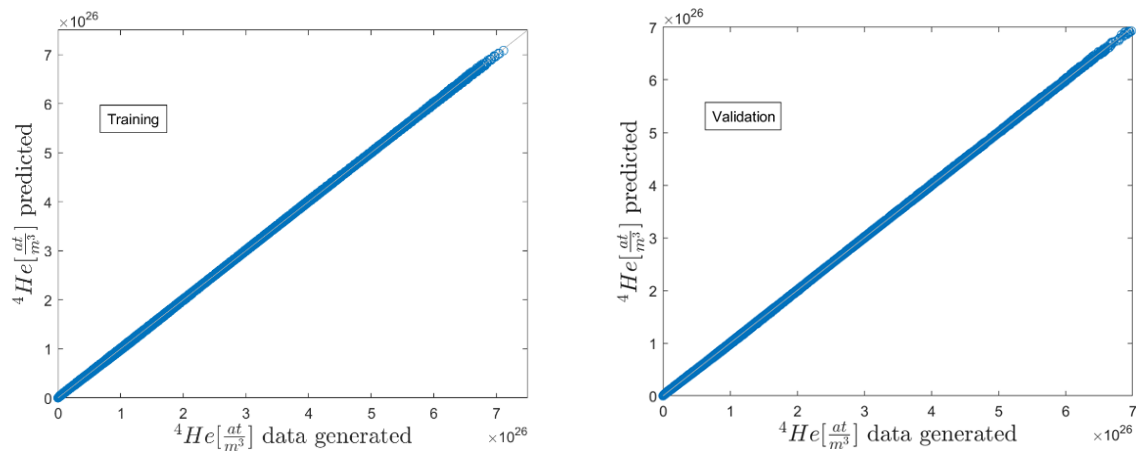


Fig. 9. Scatterplot of the predicted values of helium produced from the model proposed in this work against the values generated by the SCIANTIX burnup module (left: “training” dataset, right: independent “validation” dataset).

3.2 Helium behaviour

Given the importance of helium behaviour in fast reactor and storage conditions, mechanistic rate-theory models have been developed, implemented and validated for both its intra- and inter-granular behaviour [10], [67], [68], [98]. This section describes model and parameters currently available in the new SCIENTIX 2.0 version to describe the helium behaviour, that follows essentially the work of Cognini et al. [10] for what concerns the intra-granular helium, while recent advances on the consideration of inter-granular helium are published in [98].

3.2.1 Intra-granular helium behaviour

The helium behaviour modelling follows first its intra-granular dynamics according to the same approach adopted for the fission gases Xe and Kr [8], [32], [55], but accounting for the specificities of helium in some of the model parameters / features. To provide a satisfactory and applicable helium mechanistic modelling, helium solubility in nuclear fuel is considered following Henry's Law [68], [99], [100]:

$$c_{lim} = k_H p \quad (4)$$

where k_H (atoms $m^{-3} MPa^{-1}$) is the Henry's constant for the system He- UO_2 and c_{lim} (atoms m^{-3}) is the solubility achieved at a pressure p (MPa). The model for the intra-granular helium mobility follows the generalization of the Speight's rate theory [101] proposed by [21], disregarding the diffusivity of intra-granular bubbles [10]. Overall, the formulation for the intra-granular helium behaviour reads:

$$\begin{cases} \frac{\partial c_{He}}{\partial t} = D_{He} \frac{1}{r^2} \frac{\partial}{\partial r} r^2 \frac{\partial}{\partial r} c_{He} - g c_{He} + \gamma m_{He} + yF \\ \frac{\partial m_{He}}{\partial t} = g c_{He} - \gamma m_{He} \end{cases} \quad (5)$$

Eq. (5) shares a similar structure to the fission gas diffusion problem [8], since it includes the intra-granular helium diffusivity (Tab. 9), trapping rate, irradiation-induced and thermal re-resolution of helium atoms from intra-granular bubbles [10], [55]. Also, from the numerical point of view the problem is tackled with the spectral diffusion algorithm [102]–[104]. The suggested models of intra-granular helium diffusivities D_{He} are best-estimate correlations from the work of Luzzi et al. [67].

Table 9. Options available for helium intra-granular diffusivity ($m^2 s^{-1}$).

Option	Correlation	Reference
0	$D_{He} (m^2 s^{-1}) = 0$	–
1	$D_{He} (m^2 s^{-1}) = 2 \times 10^{-10} \exp(-24603.3)$ Best-estimate correlation for samples with no or very limited lattice damage.	[67]
2	$D_{He} (m^2 s^{-1}) = 3.3 \times 10^{-10} \exp(-19032.8)$ Best-estimate correlation for samples with significant lattice damage.	[67]

The thermal re-resolution rate of helium $\gamma (s^{-1})$ can be written as:

$$\gamma = 3D_{He} k_H k_B T Z / R_{ig,He}^2 \quad (6)$$

Z being the compressibility factor (evaluated from the Van Brutzel et al. [105] equation of state). The adopted Henry's constant for helium in UO_2 is the best-estimate correlation valid for UO_2 single crystals, hence valid for the helium inside the fuel grains, selected after the review of Cognini et al. [68]:

$$k_H = 4.1 \times 10^{24} \exp(-7543.5/T) \quad (7)$$

with a validity range for Eq. (7) between 1073-1773 K in terms of fuel temperature.

The outlined physics-based model for helium behaviour has been originally tested against five separate-effect experiments described in the work of Talip et al. [21]. These experiments represent the separate-effect validation database for helium behaviour in terms of helium release and release rate. The validation against the complete Talip's database is provided in [10] and recalled in [55]. Fig. 10 showcases the performance of the new SCIANTIX version in terms of helium release and release rate during two of the annealing experiments performed by Talip. The SCIANTIX calculations provide a promising agreement against the experimental data, despite some noticeable discrepancies. The SCIANTIX code preserves the modelling capabilities presented in the work of Cognini et al. [10] to describe the helium behaviour in nuclear fuel. Since Talip et al. annealing experiments [21] were conducted on polycrystalline samples in vacuum conditions, the model predictions are driven by the sole intra-granular helium behaviour equation – Eq. (5), neglecting the grain-boundary behaviour. Given that the model parameters (e.g., helium diffusivity) are independent from the validation database (e.g., not calibrated on Talip's experimental data), calculations provide a promising kinetic description of the helium release. Most of the differences are ascribed to the uncertainty on parameters that determines the helium thermal re-solution (e.g., the Henry's constant, for which few experimental data are available in the open literature). Nevertheless, the SCIANTIX results are coherent with the temperature history (Fig. 10 - left) and are able to catch the experimental occurrence of the double peak of He release rate (Fig. 10 - right), with the grain-boundary sweeping mechanism playing a relevant role in explaining the occurrence of the second peak [10].

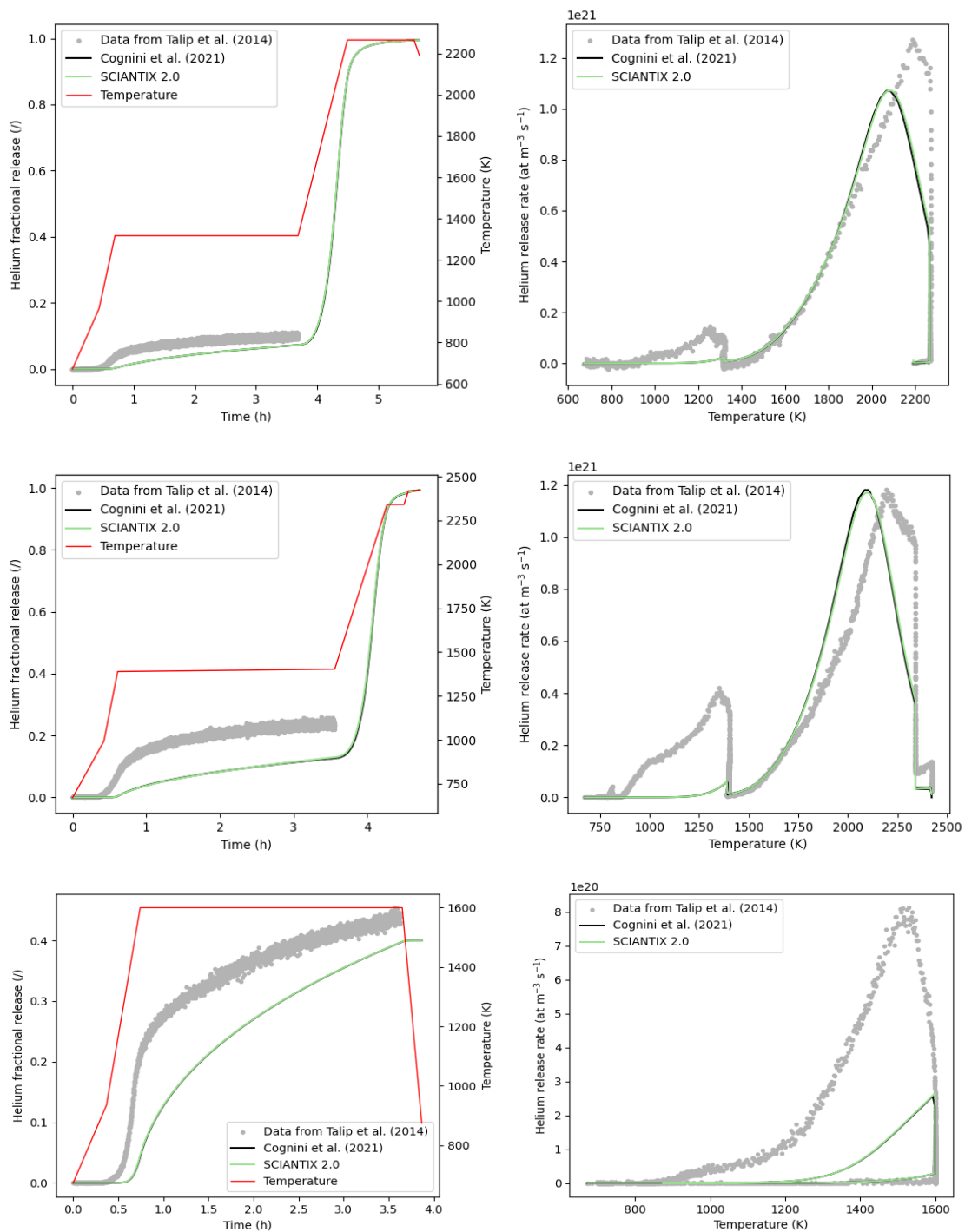


Fig. 10. Calculations of the new SCIANTIX version for helium fractional release (left) and release rate (right), against experimental data from Talip et al. [21] and original calculations by Cognini et al. [10], referred to the experimental test with the first temperature plateau at 1320 K (top) or at 1400 K (middle), or with the single plateau at 1600 K.

3.2.2 Consideration of the intra-granular behaviour of cocktails of inert gases

The physics-based models of the intra-granular behaviour of fission gases and helium are not independent of each other, but the scarcity of experimental data concerning their combined behaviour (i.e., “cocktails” of xenon, krypton and helium) hinders further model developments. For this reason, a

modelling methodology is proposed in [106], aimed at providing recommendations for accelerated experimental investigations (to be targeted by future experiments). A physics-based model was developed, extending the inert gas behaviour modelling to consider the interaction of helium and fission gas within intra-granular bubbles. The model is applied (via multiple SCIANTIX simulations) to a wide range of annealing conditions and cocktail compositions to explore the space of potential experimental conditions of interest, i.e., the full range of helium/fission gas cocktail compositions and annealing temperatures from 1000 K to 2000 K. Two conditions are considered, i.e., a low burnup set-up representative of the first weeks of fuel irradiation, and a high burnup set-up, representing highly irradiated fuel (around 100 GWd/t). The result of this wide simulation matrix is corroborated by a sensitivity analysis on the main model parameters, identified in the helium diffusion coefficient, the fission gas diffusion coefficient, the Henry's constant, the compressibility factor (involved in the Carnahan-Starling equation of state providing the partial pressure of helium within bubbles). Scaling factors are applied to these model parameters within a Pareto sensitivity analysis complementing the best-estimate SCIANTIX calculations. This work allowed to conclude that:

- The interaction between helium and fission gas is potentially relevant, with highly non-linear impact on both helium and fission gas release, at both low and high burnup. Nevertheless, the interaction is not expected to be strong in several combinations of cocktail composition/temperatures, e.g., at low annealing temperatures for every composition of the gas cocktail in intra-granular bubbles.
- Despite the coupling between helium and fission gas is connected directly to the co-presence of these species within intra-granular bubbles, the impact of the compressibility factor on their release is minimal compared to the impact of trapping and thermal re-resolution of helium, at least in the range of conditions explored in this analysis. These phenomena govern the relative quantity of helium and fission gas blocked in intra-granular bubbles and therefore not available for diffusion towards the grain boundaries.

The iterative application of this methodology in synergy with an experimental campaign can provide valuable information to focus the experimental effort, with a more efficient use of resources. On the other hand, the results of such designed experiments are going to be effective in providing feedbacks to the proposed physics-based model, both in terms of model development and validation.

3.2.3 Inter-granular helium behaviour

The consideration of the inter-granular gas behaviour may be of interest as coupled to the intra-granular dynamics, depending on the targeted experimental conditions. For this reason, research efforts have been spent on a mechanistic model for the treatment of helium behaviour at the grain boundaries in oxide nuclear fuels, published in [98]. The model, paired with the rate-theory description of the helium intra-granular behaviour described above [10], provides a rate-theory description of helium inter-granular behaviour, considering its diffusion towards grain edges, the trapping in lenticular bubbles, and thermal re-resolution. Compared to the intra-granular helium model, additional parameters are included in the master equations of the inter-granular model:

- The source of helium single-atoms coming from within the fuel grain, representing the connection between the grain boundary evolution and the intra-granular behaviour. To express this source term coherently, the intra-granular concentration helium single-atoms needs to be rescaled on a 2D space by means of the surface-to-volume ratio of the spherical grain (which is equal to one third of the spherical grain radius itself).
- The solubility of helium at the grain boundary, follows Henry's law and leading to a thermally activated re-resolution of the helium single-atoms from grain-boundary bubbles.

- The fractional coverage of the grain faces by inter-granular bubbles, acting as a parameter that distributes the helium reaching the grain boundary among the inter-granular bubble and the single-atom contributions.

The overall (intra- and inter-granular) model validation is performed against the Talip's database [21] already exploited for the intra-granular model validation, composed by thermal desorption experiments performed on ^{238}Pu (α -emitter)-doped UO_2 samples annealed at different temperatures. The overall agreement of the new model with the experimental data is improved, both in terms of integral helium release and of the helium release rate, as shown by Fig. 11. By considering the contribution of helium at the grain boundaries, it is possible to represent the kinetics of helium release rate at high temperature. Given the uncertainties involved in the initial conditions for the inter-granular part of the model and the uncertainties associated to some model parameters for which limited lower-length scale information is currently available, such as the helium diffusivity [67], [107] at the grain boundaries, the results are complemented by a dedicated uncertainty analysis. This assessment demonstrates that the initial conditions (initial helium amount at grain boundaries, helium sub-division between inter-granular solution and bubbles, helium diffusivity), chosen in reasonable ranges, have limited impact on the results, and confirms that it is possible to achieve satisfying results using sound values for the uncertain physical parameters. This corroborates the reliability of the proposed physics-based model and its validation results, although one should be cautious in generalizing the conclusions outside of the current model validation conditions (i.e., annealing, awaiting for additional experimental campaigns on irradiated fuels).

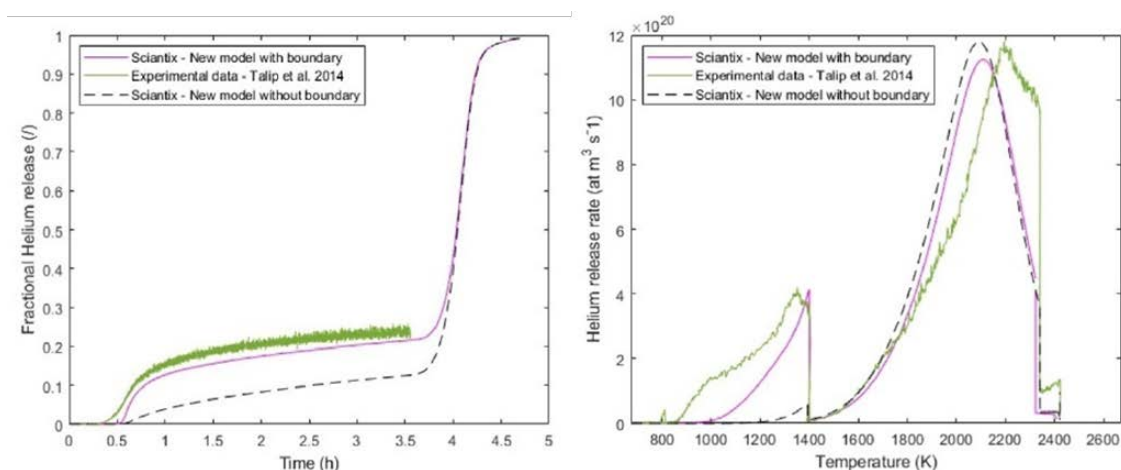


Fig. 11. SCIANTIX results for helium fractional release (left) and release rate (right), obtained via the inter-granular model coupled to the intra-granular one [98], against experimental data from Talip et al. [21] and original calculations by Cognini et al. [10] (experimental test with the first temperature plateau at 1400 K).

3.2.4 Effect of grain size distribution on helium behaviour

As a last modelling advancement applied to helium behaviour, the consideration of the actual distribution of grain sizes in specific fuel samples has been accounted for [23]. Indeed, physics-based meso-scale models of inert gas behaviour for fuel performance codes currently consider only the average grain size as physical parameter to describe the fuel microstructure [69], [70], [108], which affects the intra-granular fission gas behaviour in three ways, i.e., (1) increasing the average diffusion distance for gas atoms generated in the grains, thus hindering gas transport to the grain boundaries, (2)

through grain boundary sweeping, which provides an additional mechanism for the collection of gas atoms at the grain boundaries [5], [20], [109], and (3) by affecting the surface-to-volume ratio of fuel grains and consequently their gas storing capacity [5]. Nevertheless, information on the grain-size distribution is available for several metallographically-characterized fuel samples, e.g., from [110]. Moreover, it is known that smaller fuel grains have higher diffusion rates with respect to the bigger ones and this can bring to unbalanced gas kinetics during irradiation or annealing, that leads to a different gas release dynamics in time [111], [112]. Thus, modelling this physical effect can refine the state-of-art modelling of inert gas in fuel performance codes. In addition, this refinement allows building a relation between fuel physical properties at the nano-scale and macroscopic properties, whose understanding is fundamental for the safety and efficiency of nuclear fuel [113].

Hence, a methodology is proposed to model the effects of grain distribution on helium behaviour in polycrystalline oxide fuel samples [23]. This methodology is intended to extend the previous work by Millett et al. [110] by including a non-zero Dirichlet boundary condition, which is critical in view of the high solubility of helium in oxide fuels, and to be applicable to potentially any grain-size distribution. The multi-grain analysis performed is supported by new experimental data, obtained on samples helium-infused and annealed for which the characterization of the grain-size distribution is available in all the experimental steps [114], [115]. The detailed description of the experimental samples is provided in [23], while the methodology consists of three steps: (1) Acquisition of the empirical grain distribution from sections of the polycrystals, (2) Calculation of the gas distribution factor pertaining to each grain size class after helium infusion, and (3) Simulation of the experimental annealing histories with input parameters weighted by the gas distribution factors. To perform the multi-grain analysis the SCIANTIX code is used: each simulation run represents the infusion of helium inside each grain size class, hence it allows calculating the helium kinetics within fuel grains of a certain size. The overall problem thus formally consists in a set of diffusion equations solved for each of the grain-size classes considered, with the helium solubility is estimated for the specific experimental samples, for the most dedicated possible application of the methodology.

As a showcase of results for this activity, Fig. 12 presents the results on helium released during annealing. For what concerns fractional helium release (Fig. 12 - left), the inclusion of the grain-size distribution via the proposed methodology slightly anticipates the onset of helium release with respect to the simulation with average grain size. This is due to the small grains from which helium is released earlier due to the higher diffusion rate with respect to the average grain size. Nevertheless, from the integral point of view of total release, the effect is minimal. As for the release rate profiles (Fig. 12 - right), by applying the proposed methodology it is expected to have the peak of helium release rate at lower temperatures, i.e., closer to the experimental data compared to the simulation adopting average grain size. Complementary, the high temperature tail of the release rate peak predicted accounting for the grain-size distribution is lower than the one based solely on the average grain size, since the bigger grains exhibit a lower diffusion rate. The overprediction of the temperature at which the peak of release rate occurs could be ascribed to a slight change in stoichiometry of the samples as they are annealed at high temperatures. The results of Yakub et al. [116] indicate that the activation energy of helium diffusion in oxide nuclear fuel decreases as the matrix composition departs from stoichiometry (i.e., oxygen-to-metal ratio $O/M = 2.00$). By analysing the non-dimensional ratio $EA/k_B T$, (with EA (J) being the activation energy of helium diffusion, k_B (J/K) Boltzmann's constant, and T (K) the temperature) we can see that for the model to match the experimental release temperature of ≈ 1200 K, instead of the predicted ≈ 1400 K, the activation energy of helium diffusion should drop by $[(1200 \text{ K} - 1400 \text{ K})/1200 \text{ K}] = -14\%$, which according to Yakub et al. is compatible with a deviation of stoichiometry of $0.01-0.02$, i.e., $UO_{1.98-1.99}$. This consideration calls for the importance of controlling/assessing the samples stoichiometry in these types of experimental works. As a quantitative indication of the impact of this parameter, Fig. 12 also reports the results obtained accounting for the effect of the deviation from stoichiometry on the

activation energy of helium diffusivity, and clearly shows how this helps in correctly predicting the available experimental data on both He fractional release and release rate.

These results showcase that modelling the effect of the grain-size distribution helps predicting helium behaviour with physical coherence with respect to simply considering an average grain size (state-of-the-art approach), without a considerable impact on the computational time. Besides the effect herein described, the general overprediction of the temperature at which helium release starts could be ascribed to the helium retained at grain boundaries, which is released with lower activation energies, or to the release of helium stored close to the sample surfaces as a result of the infusion process, whose treatment is not herein considered and is targeted as a further development of this work.

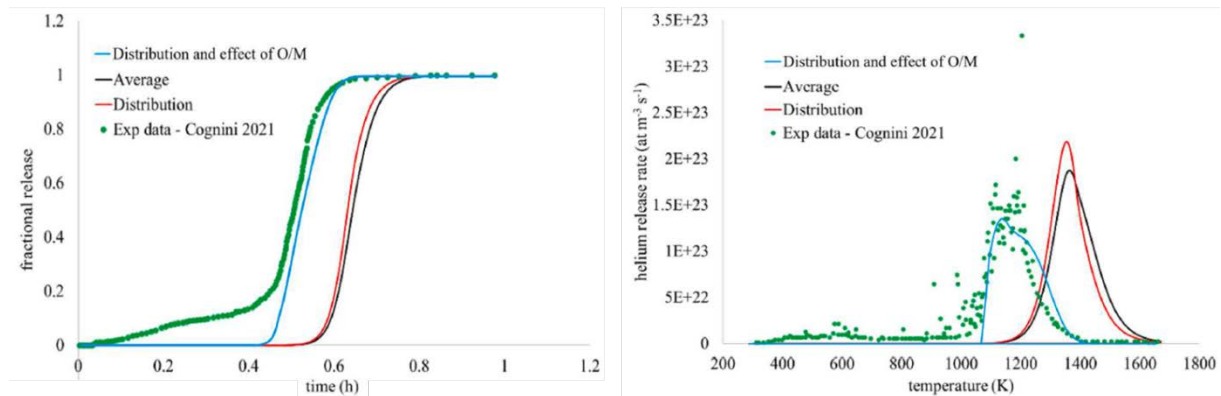


Fig. 12. Comparison of fractional helium release (left) and helium release rate (right) with experimental data from sample B12 [23]. The red curve corresponds to the SCIANITX result obtained with the proposed methodology, including the grain-size distribution effect, while the black curve is the SCIANITX result obtained by adopting the average grain size. The light-blue curve shows the effect on the results of the deviation from stoichiometry.

4 Coupling of SCIANTIX with fuel performance codes

As previously mentioned, besides the stand-alone code capabilities shown in Section 3, SCIANTIX is also designed as an intermediate-scale (grain-scale) code dedicated to inert gas behaviour to be coupled with fuel performance codes, to bridge lower length-scale calculations with the engineering-scale of the fuel and pin performance.

Concerning the inclusion/coupling of SCIANTIX within/with FPCs as an IGB module, at present the coupling with TRANSURANUS and GERMINAL is achieved and in place [48], [49], [51], [52], and demonstrated via simulations and assessments against both fast reactor irradiation experiments [52] and Generation IV reactor designs [51], [117]–[119].

The PATRICIA Project [90] foresees the application and assessment of FPCs//SCIANTIX couplings to irradiation experiments of Am-bearing oxide fuels (SPHERE, MARINE [120]–[122]) and to Am-MOX irradiations in MYRRHA “Revision 1.8”, encompassing both normal operation and transient conditions and focusing especially on the helium behaviour. These will be the focus of next PATRICIA deliverables, i.e., D5.3, D5.4, D6.1, D6.2 (pertaining to Work Packages 5 and 6 of the Project). This Section outlines the strategy and methodology related to the coupling of SCIANTIX with TRANSURANUS and GERMINAL (the two FPCs mainly involved in PATRICIA), as a basis for simulation results and analyses which are left to the mentioned following deliverables.

For both TRANSURANUS and GERMINAL FPCs, the coupling scheme in place with SCIANTIX now involves the new version 2.0 and hence includes all the extended modelling capabilities described in Section 3. The coupling involves the call of SCIANTIX at each mesh point, during each time-step, and at each convergence iteration. For each of these calls, SCIANTIX updates the physics-based variables related to inert gas behaviour, either internally or by transferring the updates to the external fuel performance code (acting as the parent code / external driver for the meso-scale module – right side of Fig. 1). The general flow of information between the two fuel performance codes and SCIANTIX is sketched in Fig. 13, with SCIANTIX receiving as inputs the local fuel temperature, the local fission rate, the local hydrostatic stress, and the time-step, and providing as outputs the local contribution to the integral fission gas release and the local gaseous swelling. These two outputs are directly connected to the overall thermal-mechanical behaviour of the fuel pin.

In the following, specificities of the coupling with / integration of SCIANTIX are provided separately for what concerns TRANSURANUS and GERMINAL.

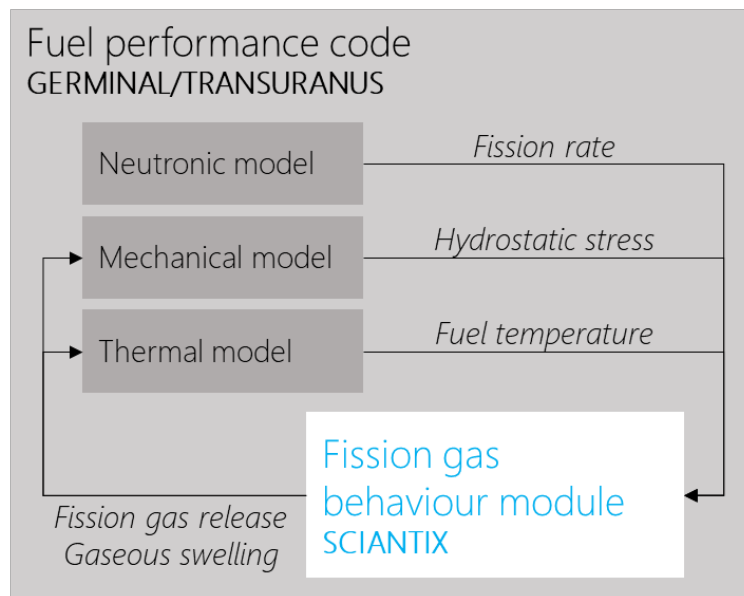


Fig. 13. Sketch of the coupling scheme between GERMINAL/TRANSURANUS and SCIENTIX [51].

4.1 Coupling of SCIENTIX with TRANSURANUS

The TRANSURANUS fuel performance code [38], [97] approximates the pin performance with an azimuthal-symmetric, axially-stacked, one-dimensional radial representation (typically referred to as 1.5D). The fuel pin is therefore discretized in axial slices and in radial coarse zones for the evaluation of the material properties (accounting for e.g., the radial temperature profile in the fuel). Each coarse zone is in turn divided into finer zones to perform the numerical integrations needed for the thermal-mechanical analysis. TRANSURANUS is designed to reflect this structure and discretization, hence it is composed by [39]:

- A main code loop for the analysis of the fuel pin behaviour at different times
- A sub-loop for the analysis of the different axial pin slices (or sections) at a specific time
- A third nested calculation loop to obtain the radial solutions of the various non-linear problems in each section or slice
- Driver programs called at each axial-radial discretization node for the various model options (e.g., for inert gas behaviour).

Consequently, the whole code is designed in levels, the three most important of which are given in Fig. 14, highlighting where (as an example of gas-related code model) the fission gas release models are called. In general, the physical phenomena governing the behaviour of the nuclear fuel pin under irradiation are included in the third level of the overall thermal-mechanical analysis, and encompass a wide set of inter-related processes mainly driven by the local fuel temperature, fission rate density, and applied stress. In the third level of the code, a specific call of the TRANSURANUS fission product behaviour models (named “FISPRO”) is thus performed, as illustrated in Fig. 15.

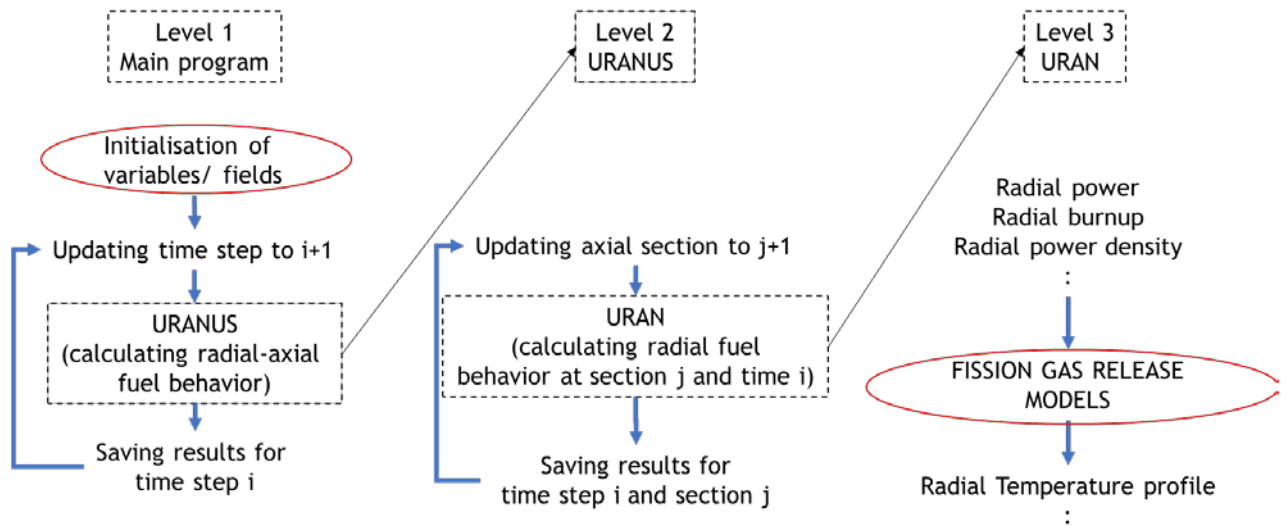


Fig. 14. Schematic flowchart and level structure of the TRANSURANUS code [97].

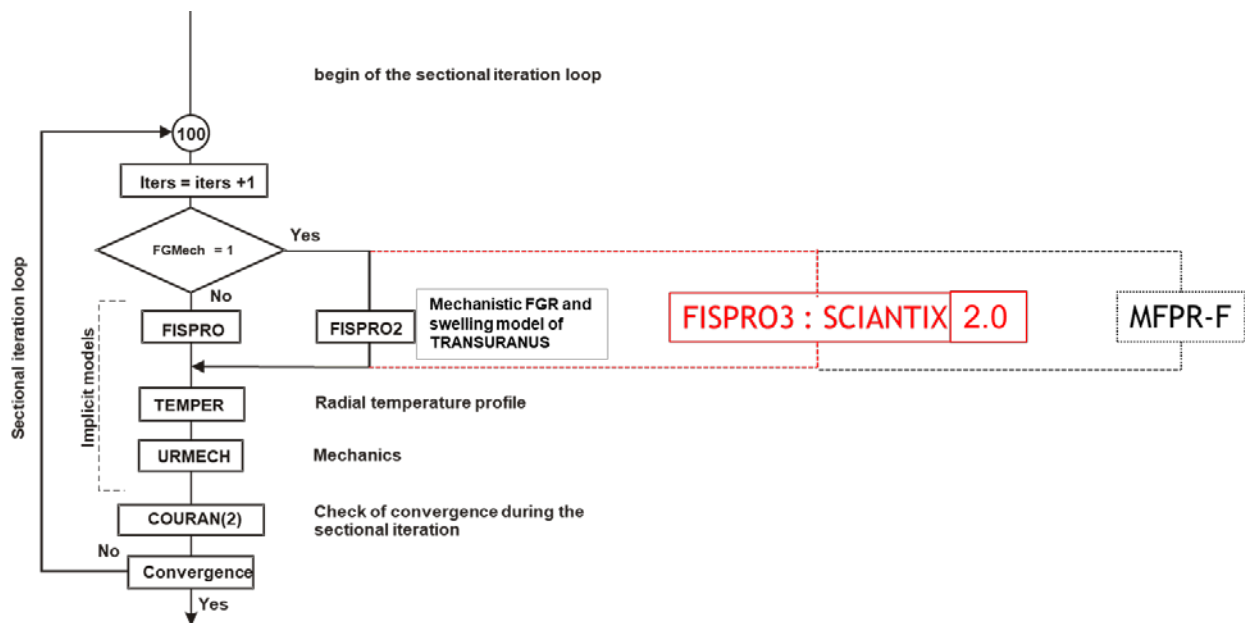


Fig. 15. Schematic flowchart of the level 3 of TRANSURANUS, driving the analysis of the fuel rod behaviour in a section or slice. The expansion of the flowchart shows the call to the different fission product behaviour models available in TRANSURANUS, among which FISPRO3 corresponds to SCIANTIX.

For the coupling of TRANSURANUS with SCIANTIX, an application program interface (API) has been developed to enable its external call and use as alternative to the standard FISPRO model of TRANSURANUS or to the mechanistic model (FISPRO2) directly embedded in TRANSURANUS [5], [123]. The API is also needed since the SCIANTIX code is programmed in C++ (object-oriented) language, whereas TRANSURANUS in Fortran. The interface for the code coupling therefore relies on the BIND(C) attribute and on the ISO_C_BINDING module of Fortran. The BIND(C) attribute enables C calling conventions and changes symbol names. The ISO_C_BINDING module provides access to named constants representing types of data representations compatible with the C types, thereby smoothing the inter-operability between the two languages.

More precisely, a new Fortran module (`fc_fdef`) has been implemented for TRANSURANUS, which describes in Fortran language the corresponding C++ functions needed to execute SCIANTIX (i.e., enabling the SCIANTIX input reading and its calling to carry out the physical calculations) and declares the correspondence between the relevant variable types in both languages. Such module is hence included in the TRANSURANUS routines that call the SCIANTIX code features within the TRANSURANUS//SCIANTIX coupled suite. Finally, to complete the API between the two codes, a corresponding, new C++ routine (`fc_api.cpp`) that implements the same interface functions defined for Fortran but from the C++ side. This C++ routine constitutes the API for both codes together with the `fc_fdef` module.

In order to minimize the effect on the existing structure of the TRANSURANUS code and in line with the strategy adopted for the coupling with MFPR-F [47], it was decided to implement a new set of global variables (in addition to the already existing TRANSURANUS global variables, contained in the `Global_Data` module) pertaining to the quantities calculated by the SCIANTIX code, which are then casted back into the existing variables of the TRANSURANUS code. To this end, a new Fortran module `CommonData_FP3` has been introduced as an additional “global variables” module. Complementarily, two new routines have also been created to transfer arrays of variables from one code to the other (i.e., from TRANSURANUS to SCIANTIX at the beginning of the SCIANTIX call, and from SCIANTIX to TRANSURANUS at the end of the SCIANTIX calculations). On one hand, the arrays of variables to be passed to the SCIANTIX code from TRANSURANUS is handled by the new routine `SetSciantikVariablesfromTU`. The variables contain the current values (i.e., at the current TRANSURANUS time-step) of the state variables, the input settings needed by SCIANTIX (choices of modelling options), and the irradiation history conditions (local temperatures, fission rate density, hydrostatic stress, local burnup, and the time step itself). On the other hand, the same global and common variables, updated via SCIANTIX calculations, are transferred back to TRANSURANUS by the `SetTUVariablesfromSCIANTIX` routine to be used as feedbacks on the thermal-mechanical analyses of the pin. New routines are also dedicated to translate the gaseous contributions to fuel swelling into strains and updates the geometry of the analysed radial position.

Finally, the compilation of the executable of the coupled TRANSURANUS//SCIANTIX code suite can be realized with any Integrated Development Environment (IDE) or via a Makefile. The running of the coupled set of codes requires two separate input files, i.e., the standard TRANSURANUS input file containing pin-level specifications, and an additional input settings file to select the model options to be used for inert gas behaviour in SCIANTIX.

4.2 Coupling of SCIANTIX with GERMINAL

SCIANTIX is integrated in GERMINAL [42], [43] by introducing the behavioural models for stable fission gases in the multi-physics convergence loop acting on each axial slice composing the discretization adopted for a fuel pin [49]. The main effects induced by the SCIANTIX modelling of fission gas behaviour coupled to GERMINAL are linked to the gas release dynamics, that modifies the gas composition inside the fuel-cladding gap and consequently the heat transfer from the fuel pellets to the cladding. Moreover, the fuel swelling induced by the retained fission gases also contributes to modify the heat transfer between fuel and cladding by changing the gap thickness.

The coupling of SCIANTIX with GERMINAL is straightforward since the SCIANTIX code is programmed in C++ language as GERMINAL, hence the creation of a coupling interface is immediate. Following the same strategy adopted for TRANSURANUS//SCIANTIX, a specific API has been developed and is available as part of the GERMINAL code.

Compared to the TRANSURANUS//SCIANTIX coupled suite, where the SCIANTIX code is coupled to the FPC preserving all the SCIANTIX capabilities, selected SCIANTIX models are integrated in the GERMINAL calculation structure, as previously mentioned. In doing so, some adjustments are introduced in GERMINAL//SCIANTIX concerning gas and gas-related models and targeting the application to fast reactor conditions [51]. These are briefly recalled here as follows:

- Related to fission gas behaviour and release, it is necessary to account for the evolution of the grain size (i.e., the fuel micro-structure) during irradiation. Indeed, the grain boundary fixes the limit of the domain where the fission gases are diffusing. The size of the grain determines the time to diffuse to the grain boundary, and consequently impacts the estimation of the gas release. The grain growth during irradiation is usually estimated from unirradiated fuel samples using empirical correlations [69], [70], [124], essentially depending on temperature and overestimating the grain growth under fast reactor irradiations at elevated fuel temperatures. The possibility to define upper bounds limiting the grain growth in the different zones of the restructured fuel pellet – columnar grains zone, equiaxed grain zone, un-restructured zone – is thus introduced in GERMINAL//SCIANTIX. The grain growth process also impacts on the fuel swelling, since the surface of the grain determines the “covering capacity” by inter-granular bubbles, which represents the main contribution to gaseous fuel swelling [5].
- The growth of the inter-granular bubbles is limited according to an asymptotical behaviour which sets a maximum bubble size. This appears necessary particularly for fast reactor irradiation conditions, where fuel temperatures tend to be high and enhance bubble growth via gas trapping.
- In addition, physically-grounded limits are introduced in the description of the gas percolation from bubbles at the grain boundary. The estimation of the vented fraction of bubbles on the grain faces is based on [62], proposing an evaluation of the inter-granular venting probability correlated with the coverage of a grain face by inter-granular bubbles (hence, a combination of bubble density and radius). The portion of gas atoms released as they reach the grain boundary increases with the fractional coverage, which results in a self-limiting bubble coalescence and growth.

Additional adaptations performed while integrating the SCIANTIX models in GERMINAL consist in:

- Updated solver for the gas diffusion inside the fuel grain: An adapted solver handling separately the two rate-equations for the gas concentration in solution in the fuel matrix and the gas concentration in intra-granular bubbles [8] is implemented (the two-equation solver is implemented and used by default in SCIANTIX, hence also in TRANSURANUS//SCIANTIX).
- Evaluation of the gas diffusion coefficient inside the grain: the intra-granular diffusion coefficient in GERMINAL//SCIANTIX can be calculated via different approaches, i.e., the Turnbull formulation [125] with adjustable parameters; an Arrhenius law with adjustable parameters [42]; a prototypical formulation with a thermally-activated term saturating faster (hyperbolic tangent-shaped) to limit the diffusivity at high temperature. The latter is intended to compensate the observed dominance of the intra-granular bubble trapping rate at high temperatures when compared to the bubble re-solution rate, resulting in an excessive gas retention in the hottest region of the fuel pellet. The possibility to apply a global scaling factor on the gas diffusion coefficient is implemented as well.

The applicability of the coupled suite GERMINAL//SCIANTIX (accounting for the mentioned adjustments) to fast reactor irradiation conditions is already provided in [51]. It proves that the coupling of GERMINAL with SCIANTIX is generally beneficial towards a more physics-based description of fission gas dynamics

within fuel pellet up to fission gas release. In particular, the coupling significantly improves the simulations of fuel pin behaviour at intermediate power levels, i.e., irradiation conditions under which the fission gas release does not reach 100% as it happens at higher power. In these cases the fission gas release must be evaluated as precisely as possible given its impact on e.g., the gap conductance and gap pressurization, as well as its relationship with the fuel gaseous swelling and the geometrical evolution of the fuel pellet. Hence, the simulation of the fission gas behaviour at the axial extremities of fast reactor fuel pins would clearly benefit from such modelling improvements.

5 Conclusions

This Deliverable describes the development and assessment of the new version (2.0) of SCIANTIX, a 0D, open-source code designed to model inert gas behaviour within nuclear fuel at the grain scale, and its coupling with two European fuel performance codes (TRANSURANUS and GERMINAL) involved in the PATRICIA Project. Indeed, SCIANTIX is hosted online at [34], [35], and it can be used both as a stand-alone code and as a module coupled with integral pin-level codes or multi-physics environments. Following this double usability, the structure and capabilities (focusing on the helium behaviour modelling) of the SCIANTIX stand-alone code have been outlined in Sections 2 and 3, respectively, while the coupling of SCIANTIX with FPCs has been described in Section 4. Various simulation results from FPCs//SCIANTIX coupled suites will be reported in future PATRICIA deliverables.

Since the first release of SCIANTIX [32], the code architecture has been revamped and the modelling capabilities have been extended [55], [56], [72]. Each physics-based model available in SCIANTIX is published in corresponding journal articles, and the developments concerning helium production and behaviour in oxide nuclear fuels (of interest for the PATRICIA Project) have been presented together with the corresponding separate-effect validation database. In summary, the current version of SCIANTIX adopts kinetic rate-theory models to describe the evolution of inert gases (xenon, krypton and helium) within the nuclear fuel, considering fundamental intra- and inter-granular processes. This description is applied both to stable fission gas isotopes (to evaluate fission gas release and gaseous fuel swelling), and to radioactive fission gas isotopes (to evaluate the radioactive release from the fuel). Lastly, the inert gas behaviour modelling is sided with models for the fuel microstructure evolution, following the evolution of the average grain size (with capabilities to evaluate the impact of a grain size distribution) and peculiar phenomena relevant for the high burnup structure.

Given the open-source nature of SCIANTIX, international standardised qualification and quality assurance guidelines are being considered and integrated directly in the source code, e.g., concerning the code documentation via automated software documentation systems [33], [61]. In addition, the online code repository [34], [35] includes non-regression testing tools and continuous integration services that are going to be further extended and developed, to improve the process needed for future code versions and branches. The online repository also hosts the verification of the SCIANTIX numerical solvers, which facilitates separate developments concerning the numerical and physical aspects of the code.

Finally, the performance of SCIANTIX as inert gas behaviour module coupled with integral fuel performance codes is under assessment against Am-bearing oxide fuels within PATRICIA, and will be investigated further. Future activities will target the coupling with as many FPCs as possible, the assessment against more irradiation experiments (both water-cooled and liquid metal-cooled) and the application to new reactors and experiment designs. This will complement the coupled suites already in place (with the TRANSURANUS, GERMINAL, FRAPCON-FRAPTRAN, OFFBEAT FPCs) and the integral simulation cases considered up to now (referred in Section 4). Future modelling advancements will be implemented not just in the stand-alone version of SCIANTIX but also in the couplings FPCs//SCIANTIX, so that the pin performance analysis will benefit from a more advanced physics-based description of inert gas behaviour and its impact at the pin level.

6 References

- [1] T. Motta and D. R. Olander, *Light Water Reactor Materials Volume I: Fundamentals*. American Nuclear Society Scientific Publications, 2017.
- [2] T. Motta and D. R. Olander, *Light Water Reactor Materials Volume II: Applications*. American Nuclear Society Scientific Publications, 2021.
- [3] P. Van Uffelen, J. Hales, W. Li, G. Rossiter, and R. Williamson, “A review of fuel performance modelling”, *J. Nucl. Mater.*, vol. 516, pp. 373–412, 2019.
- [4] J. Rest, M. W. D. Cooper, J. Spino, J. A. Turnbull, P. Van Uffelen, and C. T. Walker, “Fission gas release from UO₂ nuclear fuel: A review”, *J. Nucl. Mater.*, vol. 513, pp. 310–345, 2019.
- [5] G. Pastore, L. Luzzi, V. Di Marcello, and P. Van Uffelen, “Physics-based modelling of fission gas swelling and release in UO₂ applied to integral fuel rod analysis”, *Nucl. Eng. Des.*, vol. 256, pp. 75–86, 2013.
- [6] T. Barani, E. Bruschi, D. Pizzocri, G. Pastore, P. Van Uffelen, R. L. Williamson, and L. Luzzi, “Analysis of transient fission gas behaviour in oxide fuel using BISON and TRANSURANUS”, *J. Nucl. Mater.*, vol. 486, pp. 96–110, 2017.
- [7] M. R. Tonks, D. Andersson, S. R. Phillpot, Y. Zhang, R. Williamson, C. R. Stanek, B. P. Uberuaga, and S. L. Hayes, “Mechanistic materials modeling for nuclear fuel performance”, *Ann. Nucl. Energy*, vol. 105, pp. 11–24, 2017.
- [8] D. Pizzocri, G. Pastore, T. Barani, A. Magni, L. Luzzi, P. Van Uffelen, S. A. Pitts, A. Alfonsi, and J. D. Hales, “A model describing intra-granular fission gas behaviour in oxide fuel for advanced engineering tools”, *J. Nucl. Mater.*, vol. 502, pp. 323–330, 2018.
- [9] G. Pastore, T. Barani, D. Pizzocri, A. Magni, and L. Luzzi, “Modeling Fission Gas Release and Bubble Evolution in UO₂ for Engineering Fuel Rod Analysis”, in: *TopFuel2018 - Reactor Fuel Performance*, 30 September - 04 October 2018, Prague, Czech Republic, 2018.
- [10] L. Cognini, A. Cechet, T. Barani, D. Pizzocri, P. Van Uffelen, and L. Luzzi, “Towards a physics-based description of intra-granular helium behaviour in oxide fuel for application in fuel performance codes”, *Nucl. Eng. Technol.*, vol. 53, no. 2, pp. 562–571, 2021.
- [11] T. Barani, D. Pizzocri, F. Cappia, G. Pastore, L. Luzzi, and P. Van Uffelen, “Modeling high burnup structure in oxide fuels for application to fuel performance codes. Part II: Porosity evolution”, *J. Nucl. Mater.*, vol. 563, 153627, 2022.
- [12] M. S. Veshchunov, V. D. Ozrin, V. E. Shestak, V. I. Tarasov, R. Dubourg, and G. Nicaise, “Development of the mechanistic code MFPR for modelling fission-product release from irradiated UO₂ fuel”, *Nucl. Eng. Des.*, vol. 236, no. 2, pp. 179–200, 2006.
- [13] M. S. Veshchunov and V. E. Shestak, “Modelling of fission gas release from irradiated UO₂ fuel under high-temperature annealing conditions”, *J. Nucl. Mater.*, vol. 430, no. 1–3, pp. 82–89, 2012.
- [14] G. Jomard, C. Struzik, A. Bouloure, P. Mailhé, V. Auret, and R. Largenton, “CARACAS : An Industrial Model for the Description of Fission Gas Behavior in LWR-UO₂ Fuel”, in: *Proceedings of 2014 water reactor fuel performance meeting / Top Fuel / LWR fuel performance meeting (WRFPM)*, 14-17 September 2014, Tokyo, Japan, no. 100154, 2014.
- [15] L. Noirot, “MARGARET: A comprehensive code for the description of fission gas behavior”, *Nucl. Eng. Des.*, vol. 241, no. 6, pp. 2099–2118, 2011.
- [16] T. J. Heames, D. A. Williams, N. E. Bixler, A. J. Grimley, C. J. Wheatley, N. A. Johns, P. Domagala,

- L. W. Dickson, C. A. Alexander, I. Osborn-Lee, S. Zawadzki, J. Rest, A. Mason, and R. Y. Lee, "VICTORIA: a mechanistic model of radionuclide behavior in the reactor coolant system under severe accident conditions", NUREG/CR-5545, SAND90-0756, Rev. 1, 1992.
- [17] J. Rest and S. A. Zawadzki, "FASTGRASS : A Mechanistic Model for the Prediction of Xe, I, Cs, Te, Ba, and Sr Release from Nuclear Fuel under Normal and Severe-Accident Conditions", Report NUREG/CR-5840, ANL-92/3, 1993.
- [18] D. Yun, J. Rest, G. L. Hofman, and A. M. Yacout, "An initial assessment of a mechanistic model, GRASS-SST, in U-Pu-Zr metallic alloy fuel fission-gas behavior simulations", *J. Nucl. Mater.*, vol. 435, no. 1–3, pp. 153–163, 2013.
- [19] J. Rest, "A model for the influence of microstructure, precipitate pinning and fission gas behavior on irradiation-induced recrystallization of nuclear fuels", *J. Nucl. Mater.*, vol. 326, no. 2–3, pp. 175–184, 2004.
- [20] M. S. Veshchunov and V. I. Tarasov, "Modelling of irradiated UO₂ fuel behaviour under transient conditions", *J. Nucl. Mater.*, vol. 437, no. 1–3, pp. 250–260, 2013.
- [21] Z. Talip, T. Wiss, V. Di Marcello, A. Janssen, J. Y. Colle, P. Van Uffelen, P. Raison, and R. J. M. Konings, "Thermal diffusion of helium in 238Pu-doped UO₂", *J. Nucl. Mater.*, vol. 445, no. 1–3, pp. 117–127, 2014.
- [22] Z. Talip, T. Wiss, E. A. Maugeri, J. Y. Colle, P. E. Raison, E. Gilabert, M. Ernstberger, D. Staicu, and R. J. M. Konings, "Helium behaviour in stoichiometric and hyper-stoichiometric UO₂", *J. Eur. Ceram. Soc.*, vol. 34, no. 5, pp. 1265–1277, 2014.
- [23] D. Pizzocri, A. Cechet, L. Cognini, A. Magni, A. Schubert, P. Van Uffelen, T. Wiss, and L. Luzzi, "A modelling methodology for the description of helium behaviour accounting for the grain-size distribution", *Nucl. Eng. Des.*, vol. 411, 112426, 2023.
- [24] E. A. Kotomin, Y. A. Mastrikov, S. N. Rashkeev, and P. Van Uffelen, "Implementing first principles calculations of defect migration in a fuel performance code for UN simulations", *J. Nucl. Mater.*, vol. 393, no. 2, pp. 292–299, 2009.
- [25] D. A. Andersson, M. R. Tonks, L. Casillas, S. Vyas, P. Nerikar, B. P. Uberuaga, and C. R. Stanek, "Multiscale simulation of xenon diffusion and grain boundary segregation in UO₂", *J. Nucl. Mater.*, vol. 462, pp. 15–25, 2015.
- [26] D. A. Andersson, P. Garcia, X. Y. Liu, G. Pastore, M. Tonks, P. Millett, B. Dorado, D. R. Gaston, D. Andrs, R. L. Williamson, R. C. Martineau, B. P. Uberuaga, and C. R. Stanek, "Atomistic modeling of intrinsic and radiation-enhanced fission gas (Xe) diffusion in UO₂±x: Implications for nuclear fuel performance modeling", *J. Nucl. Mater.*, vol. 451, no. 1–3, pp. 225–242, 2014.
- [27] M. Tonks, D. Andersson, R. Devanathan, R. Dubourg, A. El-Azab, M. Freyss, F. Iglesias, K. Kulacsy, G. Pastore, S. R. Phillpot, and M. Welland, "Unit mechanisms of fission gas release: Current understanding and future needs", *J. Nucl. Mater.*, vol. 504, pp. 300–317, 2018.
- [28] M. Bertolus *et al.*, "Linking atomic and mesoscopic scales for the modelling of the transport properties of uranium dioxide under irradiation", *J. Nucl. Mater.*, vol. 462, pp. 475–495, 2015.
- [29] Y. Miao, K. A. Gamble, D. Andersson, B. Ye, Z. G. Mei, G. Hofman, and A. M. Yacout, "Gaseous swelling of U₃Si₂ during steady-state LWR operation: A rate theory investigation", *Nucl. Eng. Des.*, vol. 322, pp. 336–344, 2017.
- [30] T. Barani, G. Pastore, D. Pizzocri, D. A. Andersson, C. Matthews, A. Alfonsi, K. A. Gamble, P. Van Uffelen, L. Luzzi, and J. D. Hales, "Multiscale modeling of fission gas behavior in U₃Si₂ under LWR conditions", *J. Nucl. Mater.*, vol. 522, pp. 97–110, 2019.

- [31] A. Scolaro, P. Van Uffelen, A. Schubert, C. Fiorina, E. Brunetto, I. Clifford, and A. Pautz, "Towards coupling conventional with high-fidelity fuel behavior analysis tools", *Prog. Nucl. Energy*, vol. 152, no. February, 104357, 2022.
- [32] D. Pizzocri, T. Barani, and L. Luzzi, "SCIANTIX: A new open source multi-scale code for fission gas behaviour modelling designed for nuclear fuel performance codes", *J. Nucl. Mater.*, vol. 532, 152042, 2020.
- [33] European Commission-Euratom, "OperaHPC Euratom Project", 2022. [Online]. Available: <https://www.operahpc.eu/>.
- [34] D. Pizzocri, G. Zullo, M. Di Gennaro, A. Magni, and L. Luzzi, "SCIANTIX code - GitHub", 2023. [Online]. Available: https://github.com/dpizzocri/sciantix_patricia/tree/sciantix.
- [35] D. Pizzocri, G. Zullo, M. Di Gennaro, A. Magni, and L. Luzzi, "SCIANTIX code - Zenodo", 2023. [Online]. Available: <https://zenodo.org/record/7310850>.
- [36] J. Y. R. Rashid, S. K. Yagnik, and R. O. Montgomery, "Light water reactor fuel performance modeling and multi-dimensional simulation", *JOM*, vol. 63, no. 8, p. 81, 2011.
- [37] H. S. Aybar and P. Ortego, "A review of nuclear fuel performance codes", *Prog. Nucl. Energy*, vol. 46, no. 2, pp. 127–141, 2005.
- [38] K. Lassmann, "TRANSURANUS: a fuel rod analysis code ready for use", *J. Nucl. Mater.*, vol. 188, no. C, pp. 295–302, 1992.
- [39] A. Magni, A. Del Nevo, L. Luzzi, D. Rozzia, M. Adorni, A. Schubert, and P. Van Uffelen, "The TRANSURANUS fuel performance code", in: *Nuclear Power Plant Design and Analysis Codes - Development, Validation and Application*, Chapter 8, pp. 161–205, 2021.
- [40] J. D. Hales, S. R. Novascone, B. W. Spencer, R. L. Williamson, G. Pastore, and D. M. Perez, "Verification of the BISON fuel performance code", *Ann. Nucl. Energy*, vol. 71, pp. 81–90, 2014.
- [41] R. L. Williamson, K. A. Gamble, D. M. Perez, S. R. Novascone, G. Pastore, R. J. Gardner, J. D. Hales, W. Liu, and A. Mai, "Validating the BISON fuel performance code to integral LWR experiments", *Nucl. Eng. Des.*, vol. 301, pp. 232–244, 2016.
- [42] M. Lainet, B. Michel, J. C. Dumas, M. Pelletier, and I. Ramière, "GERMINAL, a fuel performance code of the PLEIADES platform to simulate the in-pile behaviour of mixed oxide fuel pins for sodium-cooled fast reactors", *J. Nucl. Mater.*, vol. 516, pp. 30–53, 2019.
- [43] B. Michel, I. Ramière, I. Viillard, C. Introini, M. Lainet, N. Chauvin, V. Marelle, A. Bouloire, T. Helfer, R. Masson, J. Sercombe, J.-C. Dumas, L. Noirot, and S. Bernaud, "Two fuel performance codes of the PLEIADES platform: ALCYONE and GERMINAL", in: *Nuclear Power Plant Design and Analysis Codes - Development, Validation and Application*, Chapter 9, pp. 207–233, 2021.
- [44] Y. Sukjai and K. Shirvan, "Enhancing FRAPCON fuel performance code for physical phenomena at high temperature and high burnup", *J. Nucl. Mater.*, vol. 517, pp. 113–127, 2019.
- [45] K. J. Geelhood, W. G. Luscher, J. M. Cuta, and I. E. Porter, *FRAPTRAN-2.0: A Computer Code for the Transient Analysis of Oxide Fuel Rods*, vol. 1, no. Rev. 2, 2016.
- [46] A. Scolaro, I. Clifford, C. Fiorina, and A. Pautz, "The OFFBEAT multi-dimensional fuel behavior solver", *Nucl. Eng. Des.*, vol. 358, no. 110416, 2020.
- [47] T. R. Pavlov, F. Kremer, R. Dubourg, A. Schubert, and P. Van Uffelen, "Towards a More Detailed Mesoscale Fission Product Analysis in Fuel Performance Codes: a Coupling of the TRANSURANUS and MFPR-F Codes", in: *TopFuel2018 - Reactor Fuel Performance*, 30 September - 04 October 2018, Prague, Czech Republic, 2018.

- [48] D. Pizzocri, T. Barani, and L. Luzzi, "Coupling of TRANSURANUS with the SCIANTIX fission gas behaviour module", in: *International Workshop "Towards Nuclear Fuel Modelling in the Various Reactor Types Across Europe"*, 18-19 June 2019, Karlsruhe, Germany, 2019.
- [49] P. Van Uffelen, A. Schubert, L. Luzzi, T. Barani, A. Magni, D. Pizzocri, M. Lainet, V. Marelle, B. Michel, B. Boer, S. Lemehov, and A. Del Nevo, "Incorporation and verification of models and properties in fuel performance codes", INSPYRE Deliverable D7.2, 2020.
- [50] D. Pizzocri, L. Luzzi, T. Barani, A. Magni, G. Zullo, and P. Van Uffelen, "Coupling of SCIANTIX and TRANSURANUS: Simulation of integral irradiation experiments focusing on fission gas behaviour in light water reactor conditions", in: *International Workshop "Towards nuclear fuel modelling in the various reactor types across Europe"*, 28-30 June 2021, online, 2021.
- [51] A. Magni, D. Pizzocri, L. Luzzi, M. Lainet, and B. Michel, "Application of the SCIANTIX fission gas behaviour module to the integral pin performance in sodium fast reactor irradiation conditions", *Nucl. Eng. Technol.*, vol. 54, pp. 2395–2407, 2022.
- [52] L. Luzzi, A. Magni, B. Boer, A. Del Nevo, M. Lainet, S. Lemehov, V. Marelle, B. Michel, D. Pizzocri, A. Schubert, P. Van Uffelen, and M. Bertolus, "Assessment of INSPYRE-extended fuel performance codes against the SUPERFACT-1 fast reactor irradiation experiment", *Nucl. Eng. Technol.*, vol. 55, no. 3, pp. 884–894, 2023.
- [53] G. Zullo, D. Pizzocri, A. Magni, P. Van Uffelen, A. Schubert, and L. Luzzi, "Towards grain-scale modelling of the release of radioactive fission gas from oxide fuel. Part II: Coupling SCIANTIX with TRANSURANUS", *Nucl. Eng. Technol.*, vol. 54, no. 12, pp. 4460–4473, 2022.
- [54] G. Zullo, D. Pizzocri, L. Luzzi, F. Kremer, R. Dubourg, A. Schubert, and P. Van Uffelen, "Towards simulations of fuel rod behaviour during severe accidents by coupling TRANSURANUS with SCIANTIX and MFPR-F", *Ann. Nucl. Energy*, vol. 190, no. March, 109891, 2023.
- [55] G. Zullo, L. Luzzi, and D. Pizzocri, "The SCIANTIX code for fission gas behaviour: status, upgrades, separate-effect validation and future developments", submitted to *Journal of Nuclear Materials*, 2023.
- [56] D. Pizzocri, A. Magni, G. Zullo, and L. Luzzi, "SCIANTIX open-source code for fission gas behaviour: objectives and foreseen developments", in: *IAEA Technical Meeting on the Development and Application of Open-Source Modelling and Simulation Tools for Nuclear Reactors*, 20-24 June 2022, Milano, Italy, 2022.
- [57] EU CORDIS, "R2CA - Reduction of Radiological Consequences of design basis and design extension Accidents", 2019. [Online]. Available: <https://cordis.europa.eu/project/id/847656/>.
- [58] K. J. Geelhood, W. G. Luscher, P. A. Raynaud, and I. E. Porter, *FRAPCON 4.0: A Computer Code for the Calculation of Steady-State, Thermal-Mechanical Behavior of Oxide Fuel Rods for High Burnup*, no. PNNL-19418, Vol. 1, Rev. 2, 2015.
- [59] W. L. Oberkampf and T. G. Trucano, *Verification and validation in computational fluid dynamics*, vol. 38, no. 3, 2002.
- [60] C. J. Roy and W. L. Oberkampf, "A complete framework for verification, validation, and uncertainty quantification in scientific computing", *Comput. Methods Appl. Mech. Eng.*, vol. 200, no. 25–28, pp. 2131–2144, 2010.
- [61] D. Van Heesch, "Doxygen: Source code documentation generator tool", 2008. [Online]. Available: <http://www.doxygen.org>.
- [62] D. Pizzocri, T. Barani, L. Cognini, L. Luzzi, A. Magni, A. Schubert, P. Van Uffelen, and T. Wiss, "Synthesis of the inert gas behaviour models developed in INSPYRE,", INSPYRE Deliverable D6.4,

2020.

- [63] G. Zullo, D. Pizzocri, A. Magni, P. Van Uffelen, A. Schubert, and L. Luzzi, "Towards grain-scale modelling of the release of radioactive fission gas from oxide fuel. Part I: SCIENTIX", *Nucl. Eng. Technol.*, vol. 54, pp. 2771–2782, 2022.
- [64] L. Giaccardi, M. Cherubini, G. Zullo, D. Pizzocri, A. Magni, and L. Luzzi, "Towards modelling defective fuel rods in TRANSURANUS: Benchmark and assessment of gaseous and volatile radioactive fission product release", submitted to *Annals of Nuclear Energy*, 2023.
- [65] D. Pizzocri, M. G. Katsampiris, L. Luzzi, A. Magni, and G. Zullo, "A surrogate model for the helium production rate in fast reactor MOX fuels", *Nucl. Eng. Technol.*, vol. 55, pp. 3071–3079, 2023.
- [66] L. Luzzi, A. Magni, S. Billiet, M. Di Gennaro, G. Leinders, L. G. Mariano, D. Pizzocri, M. Zanetti, and G. Zullo, "Performance analysis and helium behaviour of Am-bearing fuel pins for irradiation in the MYRRHA reactor", submitted to *Nuclear Engineering and Design*, 2023.
- [67] L. Luzzi, L. Cognini, D. Pizzocri, T. Barani, G. Pastore, A. Schubert, T. Wiss, and P. Van Uffelen, "Helium diffusivity in oxide nuclear fuel: Critical data analysis and new correlations", *Nucl. Eng. Des.*, vol. 330, no. January, pp. 265–271, 2018.
- [68] L. Cognini, D. Pizzocri, T. Barani, P. Van Uffelen, A. Schubert, T. Wiss, and L. Luzzi, "Helium solubility in oxide nuclear fuel: Derivation of new correlations for Henry's constant", *Nucl. Eng. Des.*, vol. 340, pp. 240–244, 2018.
- [69] J. B. Ainscough, B. W. Oldfield, and J. O. Ware, "Isothermal grain growth kinetics in sintered UO₂ pellets", *J. Nucl. Mater.*, vol. 49, no. 2, pp. 117–128, 1973.
- [70] P. Van Uffelen, P. Botazzoli, L. Luzzi, S. Bremier, A. Schubert, P. Raison, R. Eloirdi, and M. A. Barker, "An experimental study of grain growth in mixed oxide samples with various microstructures and plutonium concentrations", *J. Nucl. Mater.*, vol. 434, no. 1–3, pp. 287–290, 2013.
- [71] T. Barani, D. Pizzocri, F. Cappia, L. Luzzi, G. Pastore, and P. Van Uffelen, "Modeling high burnup structure in oxide fuels for application to fuel performance codes. Part I: High burnup structure formation", *J. Nucl. Mater.*, vol. 539, 152296, 2020.
- [72] IAEA, "Safety and Performance Aspects in the Development and Qualification of High Burnup Nuclear Fuels for Water Cooled Reactors - Report of a Technical Meeting", to be published, 2023.
- [73] P. Romojaró, F. Álvarez-Velarde, I. Kodeli, A. Stankovskiy, C. J. Díez, O. Cabellos, N. García-Herranz, J. Heyse, P. Schillebeeckx, G. Van den Eynde, and G. Žerovnik, "Nuclear data sensitivity and uncertainty analysis of effective neutron multiplication factor in various MYRRHA core configurations", *Ann. Nucl. Energy*, vol. 101, pp. 330–338, 2017.
- [74] P. Romojaró, "Nuclear data analyses for improving the safety of advanced lead-cooled reactors", PhD Thesis, Universidad Politécnica de Madrid, 2019.
- [75] M. E. Meek and B. F. Rider, "Compilation of Fission Product Yields", Vallecitos Nuclear Center, 1974. [Online]. Available: <https://www.osti.gov/biblio/4279375>.
- [76] M. J. Bell, "ORIGEN-2 Code, Report ORNL-TM4397", Oak Ridge National Laboratories, 1973.
- [77] D. J. Poston and H. R. Trelle, "User's Manual - Version 1.00 for Monteburns", 1998.
- [78] S. M. Bowman, M. D. DeHart, and C. V. Parks, "Validation of SCALE-4 for burnup credit applications", *Nucl. Technol.*, vol. 110, no. 1, pp. 53–70, 1995.
- [79] J. de Troulloud de Lanversin, M. Kutt, and A. Glaser, "ONIX: an open-source depletion code", *Ann. Nucl. Energy*, vol. 151, 107903, 2021.

- [80] P. K. Romano, N. E. Horelik, B. R. Herman, A. G. Nelson, B. Forget, and K. Smith, "OpenMC: a state-of-the-art Monte Carlo code for research and development", *Ann. Nucl. Energy*, vol. 82, pp. 90–97, 2015.
- [81] P. Botazzoli, L. Luzzi, S. Brémier, A. Schubert, P. Van Uffelen, C. T. Walker, W. Haeck, and W. Goll, "Extension and validation of the TRANSURANUS burn-up model for helium production in high burn-up LWR fuels", *J. Nucl. Mater.*, vol. 419, no. 1–3, pp. 329–338, 2011.
- [82] A. Soba and A. Denis, "DIONISIO 2.0: New version of the code for simulating a whole nuclear fuel rod under extended irradiation", *Nucl. Eng. Des.*, vol. 292, pp. 213–221, 2015.
- [83] H. Akie, I. Sato, M. Suzuki, H. Serizawa, and Y. Arai, "Simple formula to evaluate helium production amount in fast reactor MA-containing MOX fuel and its accuracy", *J. Nucl. Sci. Technol.*, vol. 50, no. 1, pp. 107–121, 2013.
- [84] V. I. Tarasov, E. F. Mitenkova, and N. V. Novikov, "MFPR/R-Aided Modeling of Hydrogen and Helium Production in Nuclear Fuel", *At. Energy*, vol. 125, no. 6, pp. 370–375, 2019.
- [85] J. C. Helton and F. J. Davis, "Latin hypercube sampling and the propagation of uncertainty in analyses of complex systems", *Reliab. Eng. Syst. Saf.*, vol. 81, no. 1, pp. 23–69, 2003.
- [86] A. Cechet, S. Altieri, T. Barani, L. Cognini, S. Lorenzi, A. Magni, D. Pizzocri, and L. Luzzi, "A new burn-up module for application in fuel performance calculations targeting the helium production rate in (U,Pu)O₂ for fast reactors", *Nucl. Eng. Technol.*, vol. 53, pp. 1893–1908, 2021.
- [87] J. Leppanen, "SERPENT - a Continuous-Energy Monte Carlo Reactor Physics Burnup Calculation Code, vol. 4", VTT Technical Research Centre of Finland, 2013.
- [88] J. Leppänen, M. Pusa, T. Viitanen, V. Valtavirta, and T. Kaltiainenaho, "The Serpent Monte Carlo code: Status, development and applications in 2013", *Ann. Nucl. Energy*, vol. 82, pp. 142–150, 2015.
- [89] K. Tasaka, "JNDC Nuclear Data Library of Fission Products, second version", Japan Atomic Energy Agency Research Institute, 1990.
- [90] European Union's Horizon 2020 Research and Innovation programme, "PATRICIA - Partitioning And Transmuter Research Initiative in a Collaborative Innovation Action", 2020. [Online]. Available: <https://patricia-h2020.eu/>.
- [91] M. D. McKay, R. J. Beckman, and W. J. Conover, "Comparison of three methods for selecting values of input variables in the analysis of output from a computer code", *Technometrics*, vol. 21, no. 2, pp. 239–245, 1979.
- [92] G. Locatelli, M. Mancini, and N. Todeschini, "Generation IV nuclear reactors: Current status and future prospects", *Energy Policy*, vol. 61, pp. 1503–1520, 2013.
- [93] MathWorks, "MATLAB code", 2022. [Online]. Available: <https://uk.mathworks.com/products/matlab.html>.
- [94] S. A. Glantz, B. K. Slinker, and T. B. Neilands, *Primer of Applied Regression & Analysis of Variance, Third Edition*, 2016.
- [95] PSI, "TENDL-2021 nuclear data library", 2021. [Online]. Available: https://tendl.web.psi.ch/tendl_2021/tendl2021.html.
- [96] A. J. Koning, D. Rochman, J. C. Sublet, N. Dzysiuk, M. Fleming, and S. van der Marck, "TENDL: Complete Nuclear Data Library for Innovative Nuclear Science and Technology", *Nucl. Data Sheets*, vol. 155, pp. 1–55, 2019.
- [97] European Commission, *TRANSURANUS Handbook*. Joint Research Centre, Karlsruhe, Germany,

2022.

- [98] R. Giorgi, A. Cechet, L. Cognini, A. Magni, D. Pizzocri, G. Zullo, A. Schubert, P. Van Uffelen, and L. Luzzi, "Physics-based modelling and validation of inter-granular helium behaviour in SCIANTIX", *Nucl. Eng. Technol.*, vol. 54, pp. 2367–2375, 2022.
- [99] F. Rufeh, D. R. Olander, and T. H. Pigford, "The solubility of helium in uranium dioxide", *Nucl. Sci. Eng.*, vol. 23, no. 4, pp. 335–338, 1965.
- [100] K. Nakajima, H. Serizawa, N. Shirasu, Y. Haga, and Y. Arai, "The solubility and diffusion coefficient of helium in uranium dioxide", *J. Nucl. Mater.*, vol. 419, pp. 272–280, 2011.
- [101] M. V. Speight, "A Calculation on the Migration of Fission Gas in Material Exhibiting Precipitation and Re-resolution of Gas Atoms Under Irradiation", *Nucl. Sci. Eng.*, vol. 37, pp. 180–185, 1969.
- [102] D. Pizzocri, C. Rabiti, L. Luzzi, T. Barani, P. Van Uffelen, and G. Pastore, "PolyPole-1: An accurate numerical algorithm for intra-granular fission gas release", *J. Nucl. Mater.*, vol. 478, pp. 333–342, 2016.
- [103] G. Pastore, D. Pizzocri, C. Rabiti, T. Barani, P. Van Uffelen, and L. Luzzi, "An effective numerical algorithm for intra-granular fission gas release during non-equilibrium trapping and resolution", *J. Nucl. Mater.*, vol. 509, pp. 687–699, 2018.
- [104] G. Zullo, D. Pizzocri, and L. Luzzi, "On the use of spectral algorithms for the prediction of short-lived volatile fission product release: Methodology for bounding numerical error", *Nucl. Eng. Technol.*, vol. 54, no. 4, pp. 1195–1205, 2022.
- [105] L. Van Brutzel and A. Chartier, "A new equation of state for helium nanobubbles embedded in UO₂ matrix calculated via molecular dynamics simulations", *J. Nucl. Mater.*, vol. 518, pp. 431–439, 2019.
- [106] M. Romano, D. Pizzocri, and L. Luzzi, "On the intra-granular behaviour of a cocktail of inert gases in oxide nuclear fuel: Methodological recommendation for accelerated experimental investigation", *Nucl. Eng. Technol.*, vol. 54, pp. 1929–1934, 2022.
- [107] P. Garcia, G. Martin, P. Desgardin, G. Carlot, T. Sauvage, C. Sabathier, E. Castellier, H. Khodja, and M.-F. Barthe, "A study of helium mobility in polycrystalline uranium dioxide", *J. Nucl. Mater.*, vol. 430, no. 1–3, pp. 156–165, 2012.
- [108] M. S. Veshchunov, "On the theory of fission gas bubble evolution in irradiated UO₂ fuel", *J. Nucl. Mater.*, vol. 277, pp. 67–81, 2000.
- [109] G. Pastore, L. P. Swiler, J. D. Hales, S. R. Novascone, D. M. Perez, B. W. Spencer, L. Luzzi, P. Van Uffelen, and R. L. Williamson, "Uncertainty and sensitivity analysis of fission gas behavior in engineering-scale fuel modeling", *J. Nucl. Mater.*, vol. 456, pp. 398–408, 2015.
- [110] P. C. Millett, Y. Zhang, M. R. Tonks, and S. B. Biner, "Consideration of grain size distribution in the diffusion of fission gas to grain boundaries", *J. Nucl. Mater.*, vol. 440, no. 1–3, pp. 435–439, 2013.
- [111] P. Losonen, "On the behaviour of intragranular fission gas in UO₂ fuel", *J. Nucl. Mater.*, vol. 280, no. 1, pp. 56–72, 2000.
- [112] P. Losonen, "Methods for calculating diffusional gas release from spherical grains", *Nucl. Eng. Des.*, vol. 196, pp. 161–173, 2000.
- [113] R. Parrish and A. Aitkaliyeva, "A review of microstructural features in fast reactor mixed oxide fuels", *J. Nucl. Mater.*, vol. 510, pp. 644–660, 2018.
- [114] L. Cognini, "Investigation of helium behaviour in oxide nuclear fuel", PhD Thesis, Politecnico di Milano, 2021.

- [115] Y. Miao, T. Yao, J. Lian, J.-S. Park, J. Almer, S. Bhattacharya, A. M. Yacout, and K. Mo, "In situ synchrotron investigation of grain growth behavior of nano-grained UO_2 ", *Scr. Mater.*, vol. 131, pp. 29–32, 2017.
- [116] E. Yakub, C. Ronchi, and D. Staicu, "Diffusion of helium in non-stoichiometric uranium dioxide", *J. Nucl. Mater.*, vol. 400, no. 3, pp. 189–195, 2010.
- [117] A. Magni, M. Di Gennaro, E. Guizzardi, D. Pizzocri, G. Zullo, and L. Luzzi, "Analysis of the performance of driver MOX fuel in the MYRRHA reactor under Beam Power Jump transient irradiation conditions", submitted to *Nuclear Engineering and Design*, 2023.
- [118] B. Michel, M. Lainet, A. Magni, L. Luzzi, and D. Pizzocri, "Results of the applicative benchmark between TRANSURANUS and GERMINAL on the ASTRID case study", INSPYRE Deliverable D7.4, 2021.
- [119] A. Magni, M. Bertolus, M. Lainet, V. Marelle, B. Michel, A. Schubert, P. Van Uffelen, L. Luzzi, D. Pizzocri, B. Boer, S. Lemehov, and A. Del Nevo, "Fuel performance simulations of ESNII prototypes: Results on the MYRRHA case study", INSPYRE Deliverable D7.5, 2022.
- [120] E. D'Agata, P. R. Hania, J. McGinley, J. Somers, C. Sciolla, P. J. Baas, S. Kamer, R. A. F. Okel, I. Bobeldijk, F. Delage, and S. Bejaoui, "SPHERE: Irradiation of sphere-pac fuel of UPuO_{2-x} containing 3% Americium", *Nucl. Eng. Des.*, vol. 275, pp. 300–311, 2014.
- [121] E. D'Agata, P. R. Hania, D. Freis, J. Somers, S. Bejaoui, F. F. Charpin, P. J. Baas, R. A. F. Okel, S. van Til, J. M. Lapetite, and F. Delage, "The MARINE experiment: Irradiation of sphere-pac fuel and pellets of UO_{2-x} for americium breeding blanket concept", *Nuclear Engineering and Design*, vol. 311, pp. 131–141, 2017.
- [122] A. Gallais-During, F. Delage, S. Béjaoui, S. Lemehov, J. Somers, D. Freis, W. Maschek, S. Van Til, E. D'Agata, and C. Sabathier, "Outcomes of the PELGRIMM project on Am-bearing fuel in pelletized and spherepac forms", *J. Nucl. Mater.*, vol. 512, pp. 214–226, 2018.
- [123] G. Pastore, "Modelling of Fission Gas Swelling and Release in Oxide Nuclear Fuel and Application to the TRANSURANUS Code", PhD Thesis, Politecnico di Milano, 2012.
- [124] C. Sari, "Grain growth kinetics in uranium-plutonium mixed oxides", *J. Nucl. Mater.*, vol. 137, no. 2, pp. 100–106, 1986.
- [125] J. Turnbull, R. White, and C. Wise, "The diffusion coefficient for fission gas atoms in uranium dioxide", in: *Technical committee on water reactor fuel element computer modelling in steady state, transient and accident conditions*, 18-22 September 1988, Preston, United Kingdom, 1989.
- [126] IAEA, "ONCORE - Open-source Nuclear Codes for Reactor Analysis", 2022. [Online]. Available: <https://nucleus.iaea.org/sites/oncore/SitePages/List%20of%20Codes.aspx>.